

NASA Contractor Report 156885

Aerodynamic Penalties of Heavy Rain on a Landing Aircraft

(NASA-CR-156885) AERODYNAMIC PENALTIES OF
HEAVY RAIN ON A LANDING AIRCRAFT Final
Report (Dayton Univ., Ohio.) 72 p
HC A04/MF A01

N82-30298

CSSL 01C

G3/03

Unclass
28647

P. A. Haines

and

J. K. Luers

July 1982



National Aeronautics and
Space Administration

Goddard Space Flight Center
Wallops Flight Center
Wallops Island, Virginia 23337

NASA Contractor Report 156885

**Aerodynamic Penalties of Heavy Rain on
a Landing Aircraft**

P. A. Haines and J. K. Luers

**University of Dayton Research Institute
300 College Park Avenue
Dayton, Ohio 45469**

Prepared Under Grant No. NSG-6026

NASA

**National Aeronautics and
Space Administration**

**Goddard Space Flight Center
Wallops Flight Center
Wallops Island, Virginia 23337**

NASA DISCLAIMER

The conclusions stated herein are those of the Contractor and are not necessarily those of NASA. They are being published to direct attention to the problem of the effect of heavy rain on the aerodynamic performance of an aircraft. The theory proposed herein incorporates certain assumptions and extrapolations because suitable data do not exist. Because of this, the results and conclusions reported herein are in question. They are published, however, in the hope that other researchers will be inspired to suggest and try new theoretical approaches or experimental programs to obtain the needed verifications.

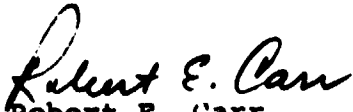

Robert E. Carr
Contract Monitor

TABLE OF CONTENTS

Section		Page
1	Exordium	1
2	Characteristics of Very Heavy Rain	3
3	Size Distribution of Water Droplets	4
4	Impingement Efficiency	8
	4.1 Overall Collection Efficiency	12
	4.2 Local Collection Efficiency	18
5	Momentum of Raindrops	19
6	Water Film	24
7	Weight Penalty	30
8	Airfoil Roughness	31
	8.1 Roughness Due to Impact	31
	8.2 Roughness Due to Film Waviness	46
	8.3 Reduction in Lift Due to Roughness	50
9	Aircraft Landings in Heavy Rain	52
10	Conclusions	61

LIST OF FIGURES

<u>Figure</u>		<u>Page</u>
1	Drop-Size Distributions by Different Rain-Rates	5
2	Percent Volume Contribution of Several Rainfall Rates by Drop Diameter	7
3	Two-Dimensional Grid of Off-Body Points for a Wing Cross-Section	9
4	Tangential Drop Trajectories for Potential Airflow About an Airfoil	13
5	Trajectories of .1mm Diameter Raindrops in Potential Flow About an Airfoil	14
6	Trajectories of 1mm Diameter Raindrops in Potential Flow About an Airfoil	15
7	Trajectories of 3.1mm Diameter Raindrops in Potential Flow About an Airfoil	16
8	Calculation of Local Collection Efficiency	18
9	Water Film Thickness Model	25
10	Water Film Thickness Model (2)	27
11	Ratio of Crown Height H to Cavity Radius at Maximum Crown Height as a Function of Weber Number	33
12	Dimensionless Crown Height as a Function of Theoretical Values from (16)	35
13	The Dimensionless Time to Reach Maximum Crown Height t^*_{crown} as a Function of the Theoretical and Experimental Values of H^* for Shallow Liquid Splashing	36
14	C_L and C_D for Configuration W, Wing Section NACA 65 A-215	44
15	C_D vs C_L for Configuration WFS Wing Section With Slat and Trailing Edge Flap	45
16	747 Landings with Momentum Penalty Only. Rain Encountered at 300 Feet	54
17	Wind Profile with Large Wind Shear	55
18	747 Landings with Drag Penalty Only. Rain Encountered at 300 Feet	56
19	747 Landings with Drag and Momentum Penalty Rain Encountered at 300 Feet	58

LIST OF TABLES

Table		Page
1	Overall Impingement Efficiency by Rainfall Rate	17
2	Force Exerted on Aircraft Due to Momentum of Drops	23
3	Average Film Thickness for a Symmetric Air- foil and Fuselage at 0 Angle of Attack, 10m Chord	29
4	Water Mass on All Aircraft Surfaces for Various Rainfall Rates	30
5	Drop Impact Parameters by Drop Size	34
6	Average Spacing Between Raindrops by Rainfall Rates	39
7	Average Geometric Height of Drop Impacts by Rainfall Rate	39
8	Sand Grain Roughnesses by Rainfall Rate	40
9	Mean Friction Coefficient for Smooth and Roughened Airfoil and Fuselage	41
10	Increase in Fatal Drag Due to Increased Wing and Fuselage Friction Drag	42
11	Equivalent Sand Grain Roughness of Wavy Water Film	47
12	Increase in Skin Friction Due to Film Waviness	48
13	Increase in Drag Coefficient Due to Film Waviness	49
14	Reduction in Maximum Lift Coefficient and Angle of Attack at Stall Due to Roughness	51
15	Summary of Landing Shortfalls (Feet) For a 747	59

FOREWORD

The research reported in this document is concerned with the aerodynamic penalties of very heavy rain. Although wind shear has been implicated as the cause of a number of aircraft crashes in landing configuration, in most cases extremely heavy rain was also present. In the accident reconstructions, no accounting for the effect of heavy rain was made and for this reason derived wind shears may be too large. This research is concerned with the frequency and intensity of very heavy rains and their effect on landing aircraft. The effects consist largely of momentum losses by the aircraft to the rain, increased drag due to roughening of the aircraft surface and decreased lift at high angles of attack due to a roughened surface. The magnitude of these effects was established by analysis of raindrop trajectories in potential flow about an aircraft and the runback of those drops impinging on the aircraft. Momentum and drag penalties were introduced into a landing simulation model. Their effect was assessed in terms of the departure of the landing touchdown point from the touchdown point for the case of no rain. The departures are also compared to those previously calculated for landings done into severe low-level wind shear.

The research was conducted by the University of Dayton Research Institute for the National Aeronautics and Space Administration, Wallops Flight Center, Wallops Island, Virginia, under the technical direction of Mr. W. E. Melson and R. E. Carr of the Engineering Division, Suborbital Projects and Operations Directorate. For the support of this effort, the authors are indebted to Mr. A. Richard Tobiason of the Office of Aeronautics and Space Technology (OAST), NASA Headquarters, Washington, D.C.

PRECEDING PAGE BLANK NOT FILMED

SECTION 1

EXORDIUM

In recent years, wind shears associated with strong thunderstorm downdrafts have been implicated as the cause of several aircraft accidents. The Eastern Flight 066 accident at Kennedy Airport (NTSB, 1976) is a prime example. In the National Transportation Safety Board's reconstruction of the flight recorder data from the accident, extraordinarily large wind shears were estimated. The reconstruction considered no other external factors besides the wind. The performance degradation due to the heavy rain cell experienced by Eastern 066 was not taken into account. We feel it possible that the derived wind shears are too large because the effect of the very heavy down-pour was ignored.

An extensive literature search revealed only one other investigation (Rhode, 1941) which considered the effect of heavy rain on aircraft performance. That investigation dealt with the case of an aircraft encountering heavy rain at moderate altitude (about 5000'). It concluded that although heavy rain has a significant effect, its exposure time is insufficient to force the aircraft to the ground. An aircraft in landing configuration, however, does not have a wide margin of performance in which to overcome the aerodynamic penalties due to heavy rain. Thus, in this report we consider the importance of heavy rain to landing aircraft.

Rain can affect an aircraft in at least four ways: (a) raindrops striking the aircraft impart a downward and backward momentum; (b) a thin water film results from the rain increasing the aircraft mass; (c) the water film can be roughened by drop impacts and surface stresses producing aerodynamic lift and drag penalties; (d) depending on aircraft orientation, raindrops striking the aircraft unevenly impart a pitching movement. In this investigation, we used recent advances in computational

fluid dynamics to assess the first three penalties. In a following report the role of rain in several aircraft accidents will be addressed.

SECTION 2

CHARACTERISTICS OF VERY HEAVY RAIN

It is first necessary to establish the nature and frequency of very heavy rain. Only short duration downpours associated with convective cells possess the intensity to seriously affect aircraft performance. We have chosen to categorize such rains by their rainfall rates in millimeters per hour.

Several authors have attempted to establish the frequency of occurrence of rainfall rates. Jones and Simms (1978) performed an analysis of one- and four-minute rainfall rates for many U.S. stations. The data used was only for a one-year period however, and the highest rate observed during that year was 238 mm/hr at Miami, Florida. Hershfield (1972) performed an analysis to obtain the expected mean maximum 5-minute rainfall rate for stations throughout the U.S. He also estimated the maximum rainfall rates over 1-minute periods to be about 50% higher than those over 5-minute periods. These results give yearly mean maximum 1-minute rainfalls of from 150 to 250 mm/hr in the eastern United States. Information about rainfall rates for periods shorter than one minute is unavailable. It is conceivable that very short period (20 to 30 second) rates are even greater than the maximum one-minute rates. Thus, the world record rainfall rate of 1828.8 mm/hr or 73.8 in/hr at Unionville, Maryland, (Riorden, 1970) suggests an upper limit of 2000 mm/hr.

A 2000 mm/hr rain will hereafter be characterized as incredible. While a 500 mm/hr rain rate is an unlikely occurrence at a single station, the chances that it will occur at one or more stations in the eastern United States each year are considerably greater. Such a rate will be termed severe. A rainfall rate of 100 mm/hr or greater is expected at least once a year in most of the eastern United States. We term this rate as heavy.

SECTION 3
SIZE DISTRIBUTION OF WATER DROPLETS

To analyze the effect of heavy rain on aircraft performance, the size distribution of water droplets under different rainfall rates must first be established. The classical paper on the size distribution of rain drops is that of Marshall and Palmer (1948). Their results show that the size distribution can be approximated by the exponential function,

$$\frac{dN(D)}{dD} = N_0 e^{-\psi D} \quad (1)$$

where $\psi = 41 R^{-0.21}$, $N(D)$ is the number of drops within diameter range dD , N_0 is an empirical constant (.0¹¹), D is the drop diameter, and R is the rainfall rate in mm/hr. The drop distributions derived from Eq. (1) for several different rainfall rates are presented in Figure 1. The distributions described by (1) were originally derived from extratropical rains but Mercerec (1975) found it valid for tropical showers as well.

The terminal velocity of raindrops of drop diameter, D , has been established by Markowitz (1976)

$$V(D) = 9.58 \left\{ 1 - \exp \left[- \left(\frac{D}{1.77} \right)^{1.147} \right] \right\} \quad (2)$$

where $V(D)$ is the terminal velocity. A correction for terminal velocity aloft is given in Markowitz

$$V(D) = V_0(D) \left(\frac{\rho_0}{\rho_a} \right)^{0.4} \quad (3)$$

where $V_0(D)$ is the terminal velocity for density ρ_0 , ρ_0 is the density aloft, and ρ_a is the density at the surface. Equation (3) allows terminal velocity adjustment for aircraft operating at higher flight levels.

It is necessary to know the percentage that each size droplet comprises of the total rain volume. The reason for this

ORIGINAL PAGE IS
OF POOR QUALITY.

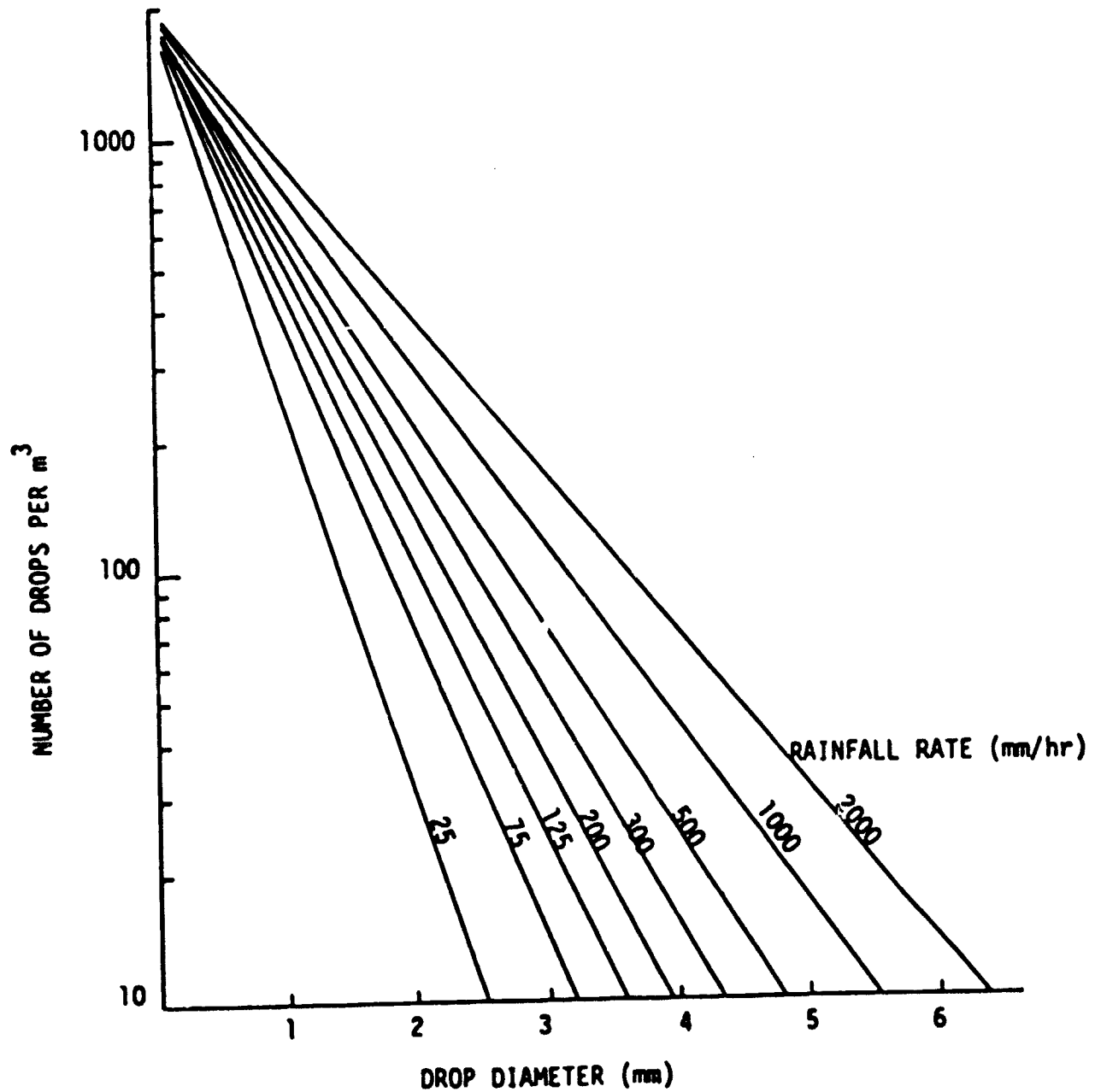


Figure 1. Drop-Size Distributions by Different Rain-Rates.

will become evident later in the impingement efficiency section. The percentage can be calculated given the terminal velocity of each size droplet and the number of droplets in each size range. Following Markowitz (1976) the frequency distribution for the fraction of total rain volume due to raindrops of diameter D is

$$M(D)dD = N(D)\frac{4}{3}\pi(D/2)^3 V(D)dD \int_0^{\infty} N(D)\frac{4}{3}\pi(D/2)^3 V(D)dD \quad (4)$$

where M(D) is the percent volume of total rain volume of drops of diameter D. Figure 2 shows the percentage volume contributions for three rainfall rates.

ORIGINAL PAGE IS
OF POOR QUALITY

— 100 mm/hr
- - 500 mm/hr
- · - · 1000 mm/hr

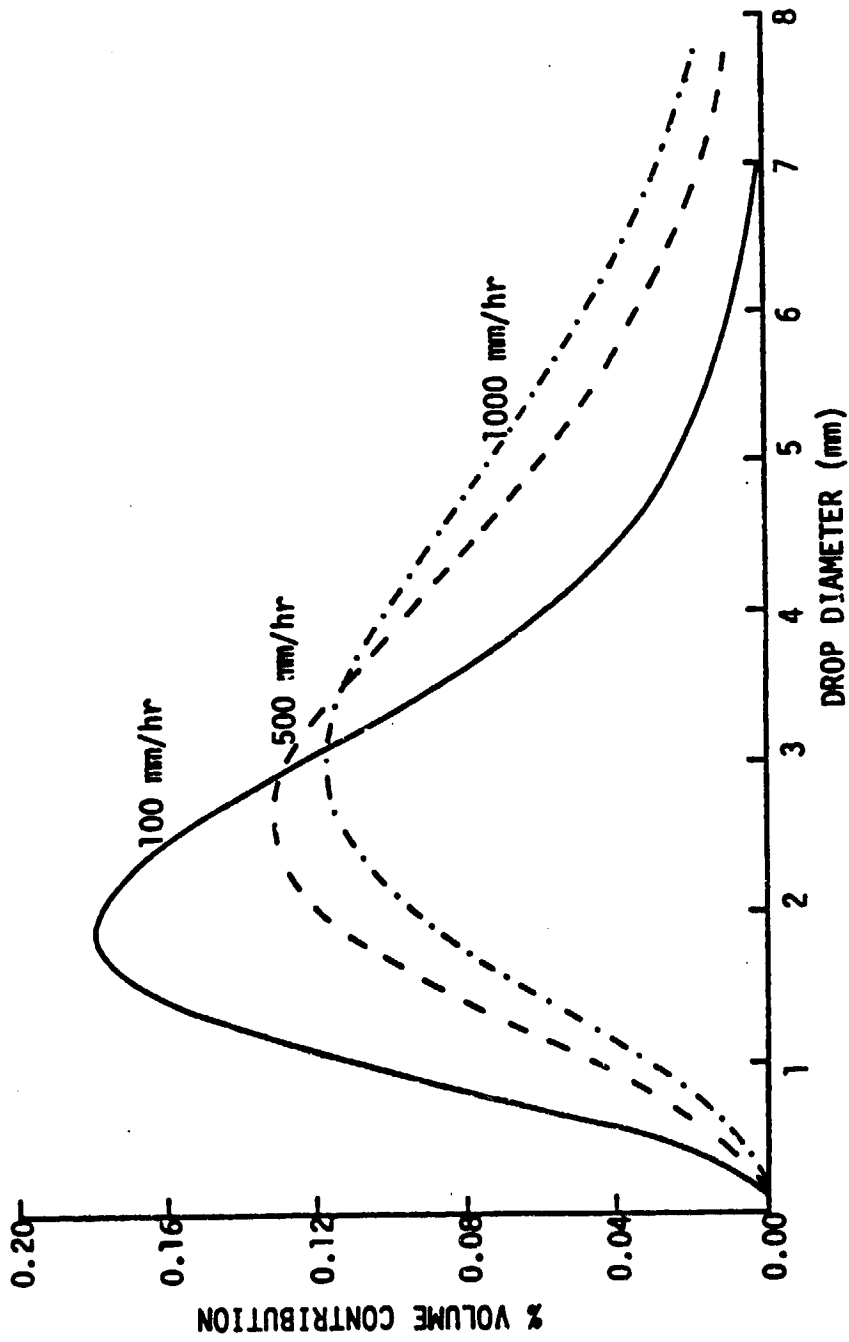


Figure 2. Percent Volume Contribution of Several Rainfall Rates by Drop Diameter.

SECTION 4 IMPINGEMENT EFFICIENCY

Obviously, not all drops in the path of an aircraft strike it. Some, especially smaller drops, are carried over the aircraft by the flow of air caused by the aircraft motion. A first step in calculating the aircraft momentum loss due to rain is calculating the ratio of the rain that strikes the aircraft to the total that would strike the aircraft in the absence of the aircraft induced airflow. This ratio is called collection or impingement efficiency.

We first calculated impingement efficiencies for a range of drop diameters from .5mm to 8mm. By knowing the relative percentage of each drop size, it was possible to establish impingement efficiencies by rainfall rate. This was done by summing the product of impingement efficiency and relative volume percentage for all drop sizes.

A water drop trajectory program together with a potential flow model were used to calculate local and overall collection efficiencies of water drops by the airfoil of an aircraft. The potential flow model calculated airflow about the airfoil. The airflow was used in calculating the paths of raindrops. The calculations were done in proximity to the aircraft for a range of drop size diameters. For momentum calculations, a summation of the products of collection efficiency times percentage contribution by drop diameter was made for each rainfall rate.

The Hess (1972) potential flow model was used because of the ease with which off-body velocities were obtained. This program has the ability to calculate the airflow about an arbitrary 3-D shape at up to 200 off-body points. These points are arranged in a two-dimensional grid so that airfoil sections are centered on the grid. The arrangement is shown in Figure 3.

ORIGINAL PAGE IS
OF POOR QUALITY

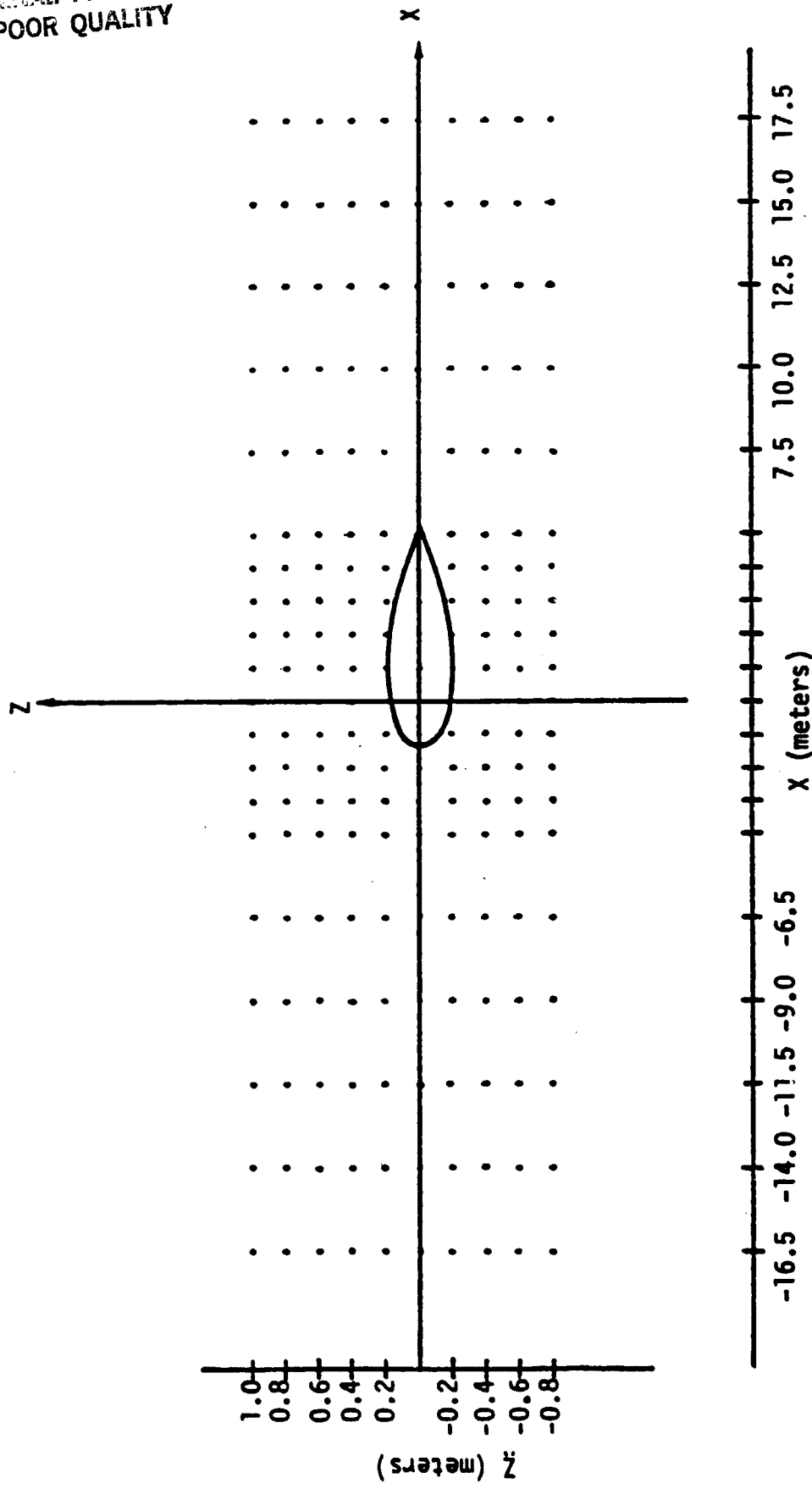


Figure 3. Two-Dimensional Grid of Off-Body Points for a Wing Cross-Section.

An arbitrary aircraft configuration is specified by geometry input which includes fuselage length and breadth, wing chord, and wing thicknesses. The angle of attack and speed may also be set arbitrarily.

Raindrops are assumed to be spherical except for very large drops for which an empirical correction for non-sphericity is applied. Their motion is governed by Newton's second law. Under the assumptions that forces acting on a drop arise solely from fluid drag and gravity and that the drop is small enough so as not to disturb the airflow field, the second law can be written as

$$m_D \frac{d\vec{U}_d}{dt} = \vec{F}_{\text{Drag}} - m_D \vec{g} \quad (5)$$

where m_D = drop mass
 \vec{F}_{drag} = drag force
 \vec{U}_d = drop velocity
 g = gravity

which expressed in non-dimensional form is (Bergrun, 1951; Norment, 1976)

$$\frac{d\vec{U}_d}{dt} = \frac{C_D Re}{24K} (\vec{U}_a - \vec{U}_d) - \vec{K}/F_N \quad (6)$$

where $Re = \rho_a D(\vec{U}_a - \vec{U}_d)V_{\text{free}}/\mu_a$ is the drop Reynold's number,

$K = 2\rho_w R_d^2 V_{\text{free}}/9\mu L$ is the inertial parameter,

$F_N = V_{\text{free}}^2/Lg$ is the Froude number,

$$\vec{U}_d = \frac{\vec{U}_d'}{V_{\text{free}}}, \quad \vec{U}_a = \frac{\vec{U}_a'}{V_{\text{free}}}, \quad t = \frac{t' V_{\text{free}}}{L},$$

ρ_a the air density,

ORIGINAL PAGE IS
OF POOR QUALITY

ρ_w the water density,

U_a the air velocity at the drop position,

V_{free} the free stream velocity,

R_d the drop radius,

L a characteristic length either the wing chord or fuselage length,

and μ is the viscosity.

The drag coefficient, C_D , is a function of the drop Reynolds's number (Walsh, 1977)

$$C_D = \frac{24}{Re} (1 + 0.15Re^{.687}).$$

For large Reynolds number, i.e., $Re > 200$, the drag must be corrected for non-sphericity of the drops. C_D is iterated in the empirical relation (Berry and Pranger, 1974)

$$\ln Re = a_{20} + a_{21} \ln X_2 + a_{22} (\ln X_2)^2 + a_{23} (\ln X_2)^3$$

where $X_2 = C_D Re^2$ $a_{20} = -0.236534 \times 10^1$, $a_{21} = 0.767787$,

$$a_{22} = 0.535826 \times 10^{-2}, \text{ and } a_{23} = 0.763554 \times 10^{-3}$$

until a solution is obtained.

Eq. (6) is integrated numerically by a 4th order Runge-Kutta scheme to obtain $\vec{U}_d(t+\Delta t)$ and drop positions are incremented by (Ackley and Templeton, 1979),

$$X_d = X_d + U_d dt$$

$$Z_d = Z_d + W_d dt$$

where X_d is the x drop position and Z_d is the z drop position. The integration of a droplet trajectory begins at a point sufficiently forward of the airfoil where the flow is unaffected by the airfoil and continues until either the droplet impacts the airfoil or passes over or under the airfoil.

4.1 OVERALL COLLECTION EFFICIENCY

The overall collection efficiency for a given drop diameter is the ratio of drops that strike the airfoil to those that would have hit the airfoil had the airflow not affected the drop trajectories. This ratio can be expressed as $E = (Z_H - Z_L)/H$ where H is the projected height of the airfoil onto the initial drop positions and Z_H and Z_L are the initial drop positions for respectively the highest and lowest drops to impact the airfoil (see Figure 4).

Some examples of trajectories in the vicinity of the wing are shown in Figures 5, 6, and 7 together with the overall collection efficiency of each drop size. The respective drop diameters for these figures are .1 mm, 1 mm, and 3.1 mm.

The overall collection efficiency by rainfall rate is obtained by summing the product of drop size collection efficiency and percent volume contribution for all size drops. The summation is done for drop diameters from .5mm to 8mm in .5mm increments.

$$CE = \sum_{i=1}^{16} E_i M(D)_i$$

where E_i and $M(D)_i$ are respectively the overall drop collection efficiency and percent rain volume of the i th size drop. Table 1 summarizes the results for a symmetric airfoil at 0° angle of attack with a 65 m/sec velocity. The overall collection efficiencies are greater than 95% for all rainfall rates of interest. Similar results would be anticipated for other airfoils and for the fuselage. Large angles of attack may decrease somewhat the overall collection efficiencies.

ORIGINAL PAGE IS
OF POOR QUALITY.

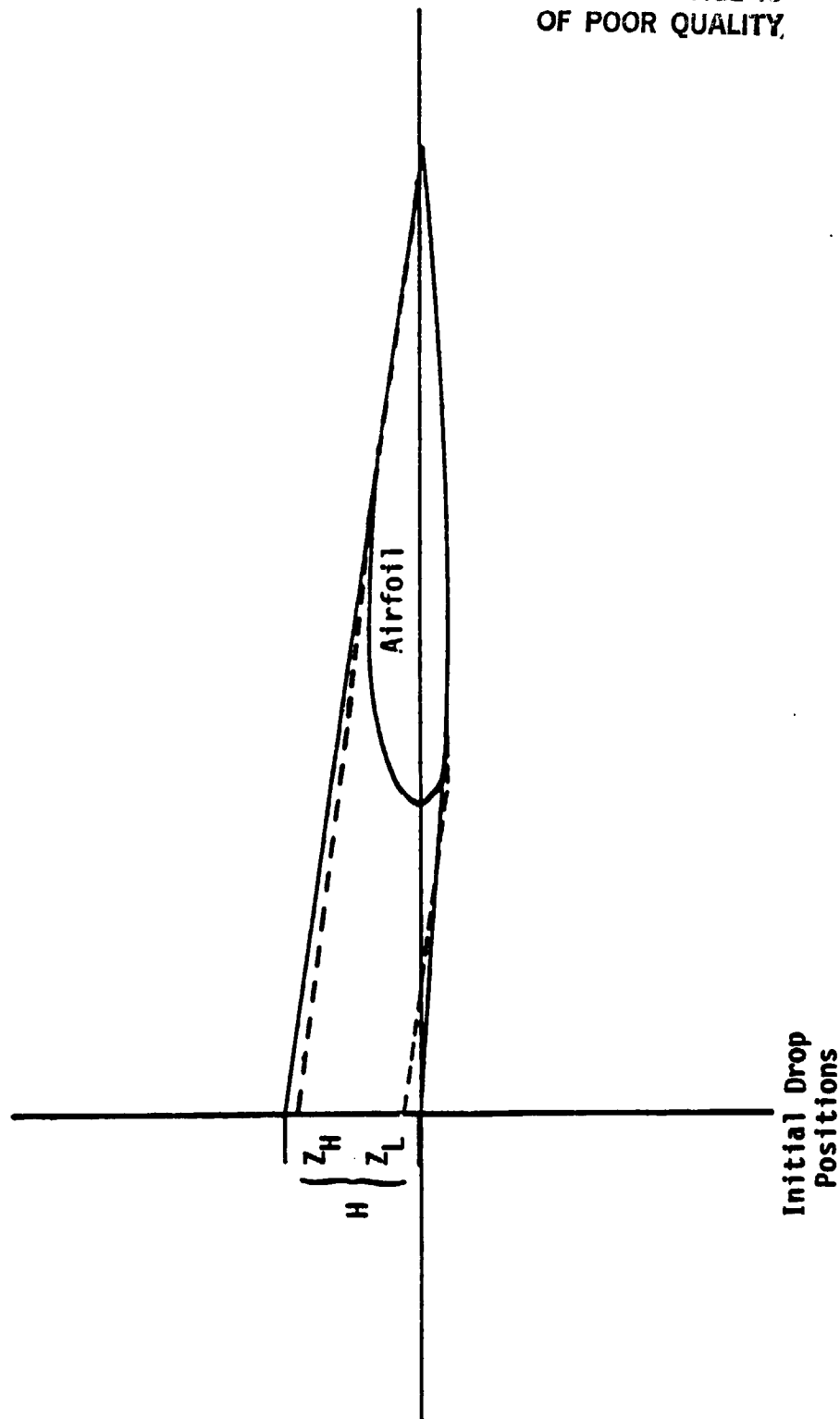
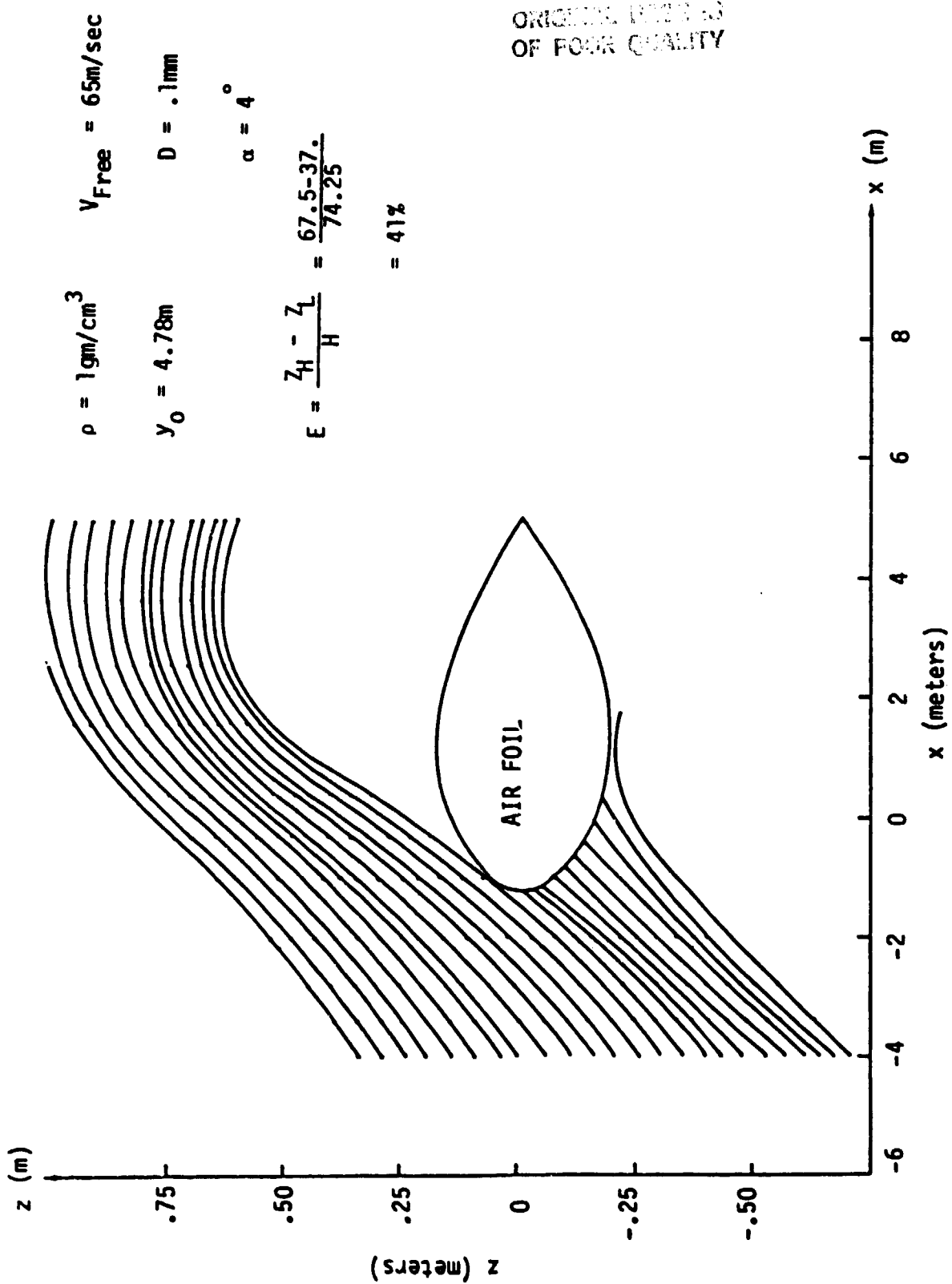


Figure 4. Tangential Drop Trajectories for Potential Airflow About an Airfoil. Drop trajectories begin well ahead of the airfoil to ensure that initially their paths are unaffected by the airflow.



ORIGINAL FIGURE IS OF POOR QUALITY

Figure 5. Trajectories of .1mm Diameter Raindrops in Potential Flow About an Airfoil. (Note: Difference in X and Z scales)

ORIGINAL PAGE IS
OF POOR QUALITY

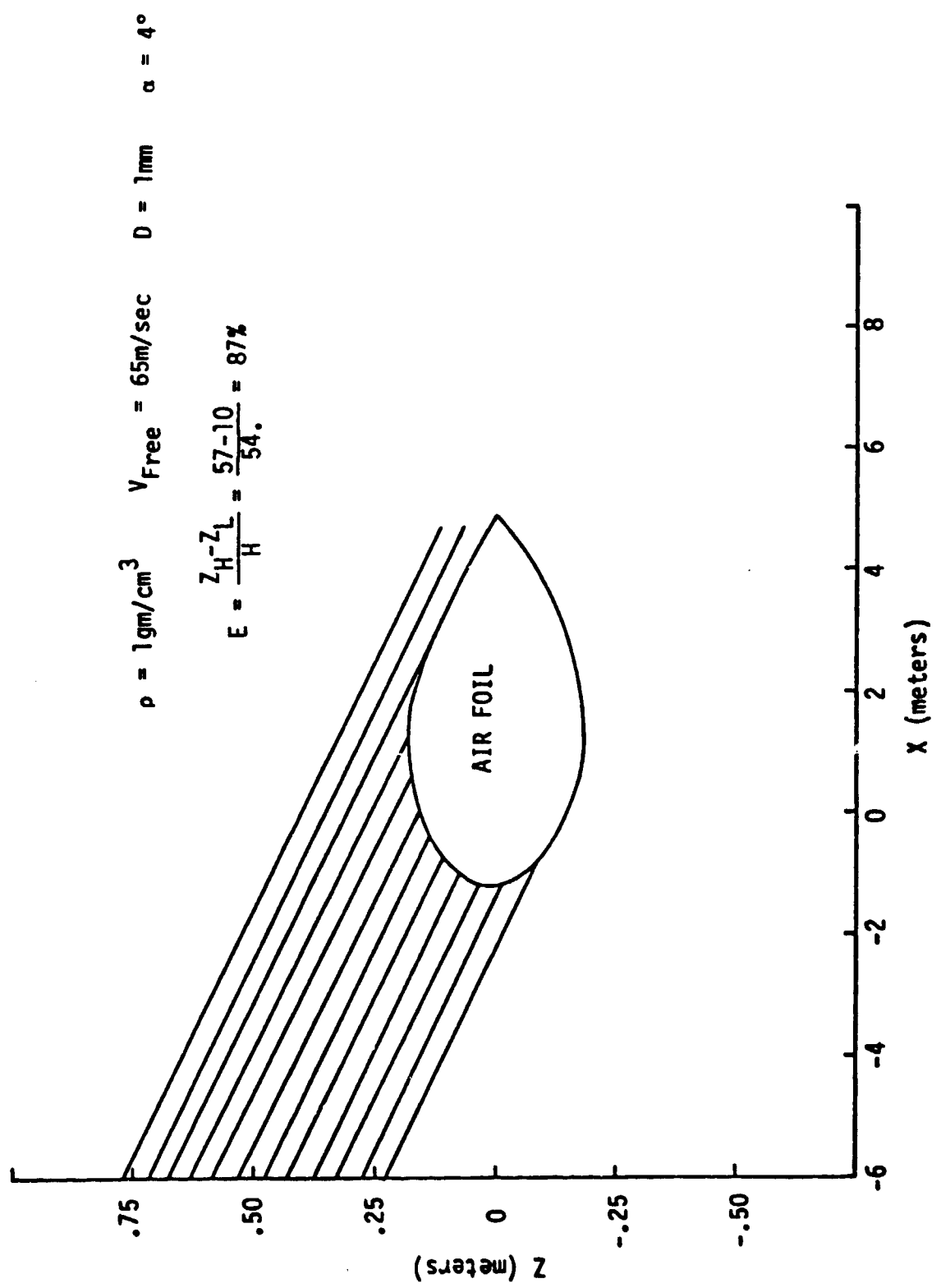


Figure 6. Trajectories of 1mm Diameter Raindrops in Potential Flow About an Airfoil.

ORIGINAL PICTURE
OF POOR QUALITY

$\rho = 1\text{gm/cm}^3$ $V_{\text{Free}} = 65\text{m/sec}$ $D = 3.1\text{mm}$ $\alpha = 4^\circ$

— WING
—•— DROP TRAJECTORY

$$E = \frac{Z_H - Z_L}{H} = \frac{139 - 55.5}{84} = 99\%$$

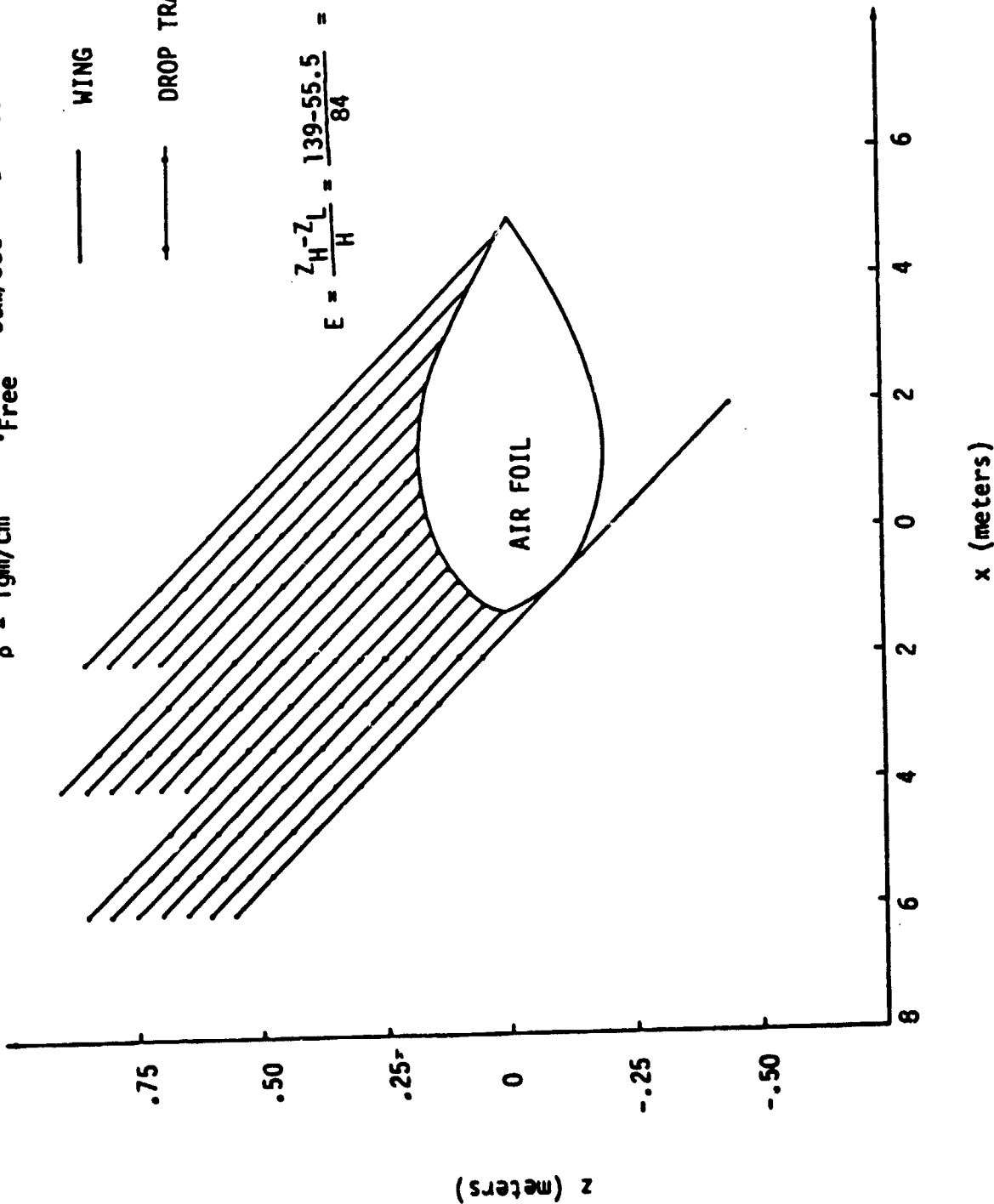


Figure 7. Trajectories of 3.1mm Diameter Raindrops in Potential Flow About an Airfoil.

TABLE 1
OVERALL IMPINGEMENT EFFICIENCY BY RAINFALL RATE

<u>Drop Diameter (mm)</u>	<u>Collection Efficiency (%) (E)</u>
0.5	78.4
1.0	87.1
1.5	95.2
2.0	96.4
2.5	97.7
3.0	99.0
3.5	99.5
4.0	99.5
4.5	99.5
5.5	100.0
6.0	100.0
6.5	100.0
7.0	100.0
7.5	100.0
8.0	100.0

$$CE = \sum_{i=1}^{16} E_i (\%Vol)_i$$

% Vol is volume contribution
of ith size drops

Rainfall Rate (mm/hr)	2000	1000	500	200	100	25
E (%)	99+	98.7	98.1	97.4	96.7	95.7

4.2 LOCAL COLLECTION EFFICIENCY

Determining where a raindrop has impacted the wing is crucial to calculating the local collection efficiency at various segments of the airfoil as well as calculating other impact parameters. Local collection efficiency is required in assessing the water film that may develop on the wing due to heavy rain in addition to assessing the roughness that may develop in the film. The local collection efficiency, β , is the initial vertical distance between successive drop trajectories, dz , divided by the distance along the wing between successive impacts, ds (see Figure 8). Using the droplet trajectory program, local collection efficiencies were calculated for each droplet diameter at various stations around the airfoil. Local collection efficiencies by rainfall rate were then established at each station by weighting the percentage volume contribution of each droplet diameter by the local collection efficiency for that diameter and summing over drop diameter.

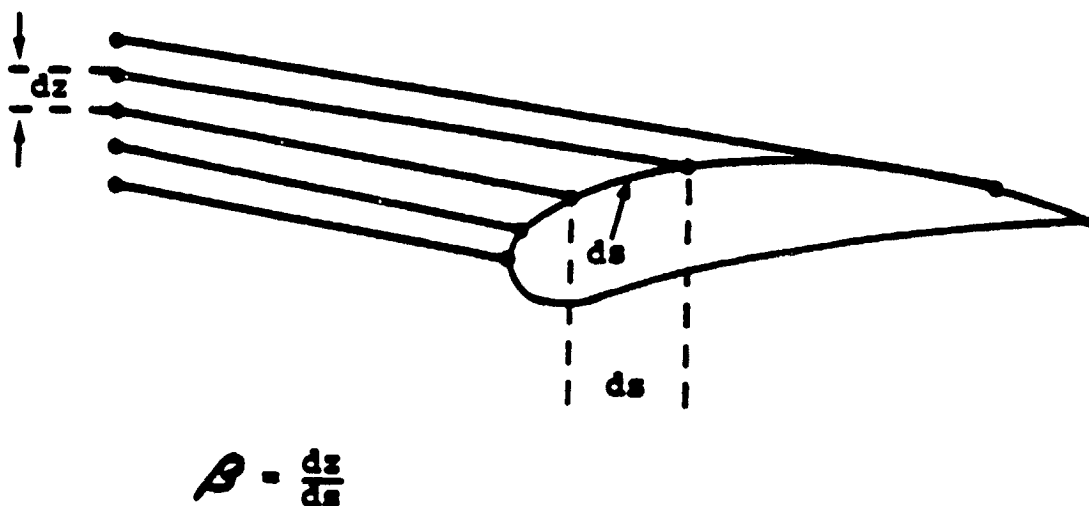


Figure 8. Calculation of Local Collection Efficiency.

SECTION 5 MOMENTUM OF RAINDROPS

Raindrops striking an aircraft lose momentum to the aircraft, thus changing the velocity of the aircraft. The vertical component of the raindrop velocity imparts downward momentum to the aircraft, which tends to make it sink. The raindrops striking head-on slow the aircraft because momentum is lost in accelerating the water droplets to the aircraft velocity. The amount of momentum imparted to an aircraft by striking a raindrop depends on the reflection angle of the raindrops. A raindrop striking the aircraft surface acutely imparts less momentum than if it strikes at a larger reflection angle. To estimate the impacted momentum for a large aircraft such as a Boeing 747, the following assumptions are made:

- (a) All rain impinging on the aircraft accelerates to the velocity of the aircraft (inelastic collision)
- (b) The aircraft is in straight and horizontal flight at zero degrees angle of attack
- (c) The flaps are not deployed
- (d) The aircraft goes from the no-rain to rain situation instantaneously.

The assumption that the rain strikes the aircraft directly and takes on its velocity is an underestimate for drops striking head on. Any reflection for these drops will be at an angle greater than 90°; thus, the impact force from the partially elastic collision of these drops is actually greater than accounted for in the inelastic calculations. Some drops striking the wing or fuselage will suffer reflection at an acute angle. The force imparted by these latter drops is less than that accounted for in the momentum calculations. The assertion that the impacts are inelastic is supported by the Lucey (1972) work on the Crush of a Point Detonating Element. The element was mounted on a rocket sled and passed through a heavy rainfield. The measured crush of the element was related to work energy and

was compared to the work that would have been done by both elastic and inelastic collisions. The comparison showed the measured crush could be best explained by inelastic collisions.

The calculation of rain-induced momentum penalties does not consider a landing wing configuration using flaps; this would present a larger impact cross-section than does a wing in horizontal flight. Likewise, a non-horizontal aircraft attitude would generally present a larger impact cross-section. A greater momentum penalty would result in both cases.

The above assumptions used in calculating momentum penalties may overestimate the effect in some areas and underestimate it in other areas. Nonetheless, we believe they exhibit sufficient realism for an initial aerodynamic assessment.

To estimate the horizontal momentum imparted to the aircraft, visualize the process as that of a water jet whose discharge is equivalent to the rainfall interception rate. The water jet hits the aircraft at the freestream speed and loses all its momentum to the aircraft. What is the force the aircraft must apply to overcome the jet?

In the horizontal x-direction

$$F_x = \dot{M} (V_{x\text{FREE}}) \quad (7)$$

where

\dot{M} is the mass interception rate of water per second, and $V_{x\text{FREE}}$ is the horizontal component of the aircraft velocity relative to the air mass. With the assumption that the final velocity of the water after impact is zero, Eq. (7) determines the horizontal force exerted on the aircraft by the rain.

The vertical force of rain impact on the aircraft is considerably less since the terminal velocity of heavy rain in still air from eq. (2) is about 9 m/sec.

In the vertical z-direction

$$F_z = \dot{M} (W_o + V_{z\text{FREE}}) \quad (8)$$

where

W_o is the vertical velocity of the drops, and

$V_{z\text{FREE}}$ is the vertical component of the aircraft velocity relative to the air mass.

The mass interception rate, \dot{M} , is given by

$$\dot{M} = |\vec{W}_R| A_p \rho_l CE$$

where

\vec{W}_R = Impact velocity vector of water drops

A_p = Projected area of the aircraft in the direction of drop impacts, \vec{W}_R

ρ_l = liquid water content of the air as a function of rainfall rate

CE = overall collection efficiency of the aircraft as a function of rainfall rate and angle of attack.

The impact velocity vector of the water drops is derived from summing the Aircraft Velocity Vector (\vec{V}_{AC}), the Wind Vector (\vec{V}_{AIR}), and Raindrop Terminal Velocity Vector (\vec{W}_o) as

$$\vec{W}_R = \vec{V}_{AC} - \vec{V}_{AIR} + \vec{W}_o.$$

The projected area A_p for an aircraft varies considerably as the view angle changes from horizontal. An accurate determination of the presented view of a specific aircraft by view angles is beyond the scope of this report. A flat surface approximation can be used to obtain the projected area as a function of view angle, given the frontal and top view surface areas.

The approximation, is

$$A_P = A_T \sin(\gamma) + A_F \sin(90^\circ - \gamma)$$

where

A_T = Top view surface area

A_F = Frontal view surface area

γ = Angle between fuselage reference line and \vec{W}_R .

Evaluation of the total force exerted on a 747 aircraft and the x and z components of this force for horizontal flight at 65 m/sec (approximately 125 knots) and 0° angle of attack is given in Table 2 by rainfall rate. The additional force needed to balance the momentum penalty can be compared with the thrust produced by the aircraft engines. For a 747 aircraft the maximum engine thrust is on the order of 800,000 newtons (180,000 lbs). Thus at a rainfall rate of 100 mm/hour only 0.4 percent of maximum thrust is needed to counteract the rain momentum while at a 2000 mm/hour rate, 9 percent of maximum thrust is required.

If no additional thrust were applied and the other forces on the aircraft remained constant then the rain momentum would extract speed from the aircraft. The resulting deceleration equals the momentum force divided by the mass of the aircraft. The deceleration for a 180,000 kg aircraft varies from .04 knots/sec for a 100 mm/hour rain to 0.2 knots/sec for a 500 mm/hour rain to 0.75 knots/sec for a 2000 mm/hour rain. If the aircraft were in the heavy rain environment for a 20 second period, the approximate resulting loss of airspeed would be 0.8 knots for the 100 mm/hour rate, 4 knots for the 500 mm/hour rate and 15 knots for the 2000 mm/hour rate. These calculations of airspeed loss could be an underestimation for a landing configuration with high lift devices extended (which increase the water catch rate) or for a landing at a higher approach velocity (larger momentum loss) or when applied to an aircraft executing a go-around maneuver (increased water catch rate). Nevertheless it

appears that significant momentum penalties result for transport class aircraft for rainfall rates of 500 mm/hour or greater. For rates less than 500 mm/hour, typical of most accident scenarios, the momentum penalty may be a contributing factor but of itself would not be expected to present severe problems. These momentum penalties are further analyzed in a subsequent section using a landing simulation program to assess their effect on aircraft performance.

TABLE 2
FORCE EXERTED ON AIRCRAFT DUE TO MOMENTUM OF DROPS

RAINRATE (mm/hr)	ρ_{lw} gm/m ³	W_o m/sec	F Newtons	F_x Newtons	F_z Newtons
100	3.23	8.42	3.60×10^3	3.57×10^3	4.57×10^2
200	6.23	8.96	7.13×10^3	7.06×10^3	9.67×10^2
500	15.31	9.14	1.82×10^4	1.80×10^4	2.62×10^3
1000	30.18	9.30	3.58×10^4	3.54×10^4	5.17×10^3
2000	59.74	9.45	7.09×10^4	7.01×10^4	1.02×10^4

B-747 Aircraft

$V_{AC} = 65 \text{ m/sec}$

$A_T = 1131 \text{ m}^2$

$A_F = 119 \text{ m}^2$

$CE = 1.0$

SECTION 6 WATER FILM

In very heavy rain, a water film forms on the upper surfaces of the wings, fuselage, and tail. The film may profoundly affect aircraft performance not only by increasing aircraft mass, but also by increasing total aircraft drag and decreasing lift. For the purposes of aerodynamic penalties, it is necessary to calculate the film's mean thickness. In order to arrive at the film thickness, a number of assumptions were made.

Because it is relatively thin and thus moves considerably slower than the airflow above it, the film is assumed to be laminar. Its primary motivation is due to the airflow. At the interface viscous stress is matched between air and water. The resulting film is a balance between water runback and rain water reception. We assume the rain water reception is not affected by droplets shedding from the drop impact crowns. The shed droplets are probably returned to the film by boundary layer entrainment.

The local rate of mass reception is required for calculating the film thickness. The reception rate is dependent on the liquid water content of the air, ρ_{lw} , the free stream airspeed, V_{free} , and the local collection efficiency β . For a given location the reception rate per unit area is given by

$$\dot{M} = \rho_{lw} \beta \vec{V}_{free}$$

A numerical model for the water film was developed to calculate film thickness by airfoil location and rainfall rate. The model geometry calculates the film flow at a number of stations along the wing as shown in Figure 9. At each station, the film thickness results from water remaining after the gains and losses due incoming rain and film flow are considered. After a time, an equilibrium thickness results at each station. A more complicated model that considers pressure gradient, gravity, and

ORIGINAL PAGE IS
OF POOR QUALITY

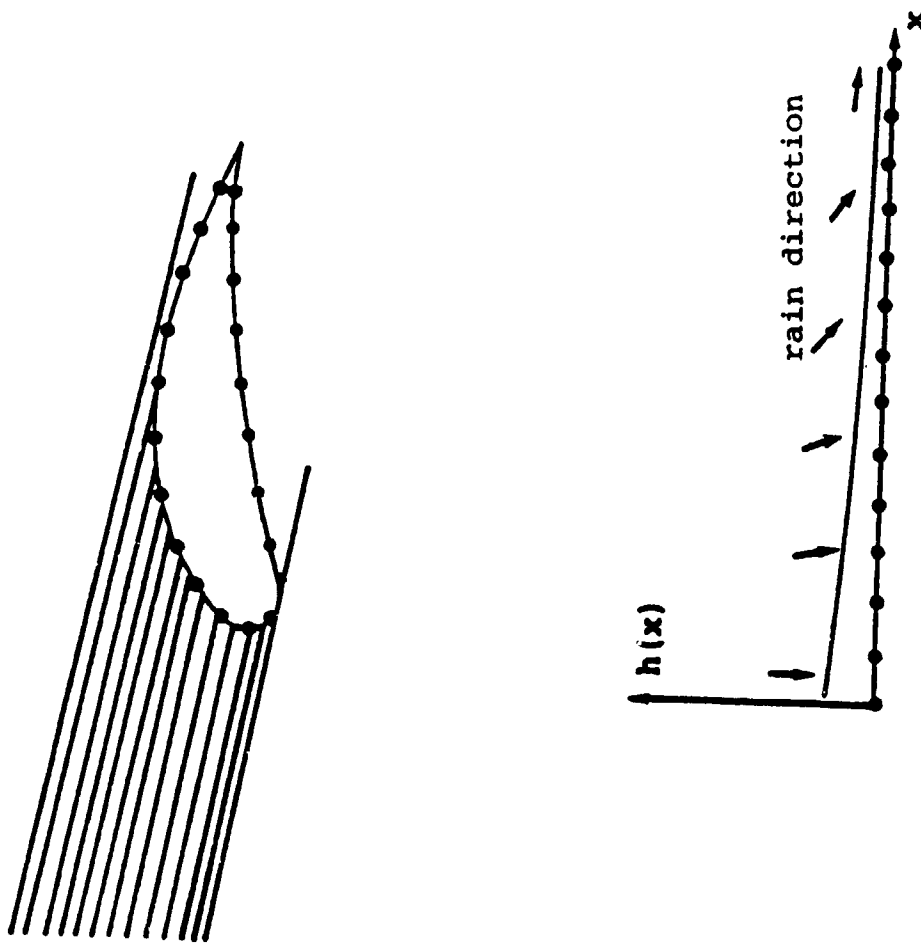


Figure 9. Water Film Thickness Model.

other effects is not warranted in a first look at heavy rain effects on aircraft. Refinements to the model may be desirable in the future however.

For simplicity, the model considers the wing to be a flat plate and the direction of the arriving rain varies from nearly normal at the leading edge to nearly tangential depending on angle of attack at the trailing edge. Slower airflow near the stagnation point is not incorporated, for this reason the calculated film thicknesses near the leading edge are probably too thin.

The model is two-dimensional and consists of computations at 100 stations shown in Figure 10. A linear velocity profile is assumed between specified velocities at the film's top and bottom. At the bottom, the film velocity is zero. At the top, the velocity is based on the viscous stress due to the airstream above the water film. Following Hartley and Murgatroyd (1964), the shear stress at the surface of the film is

$$\tau = f_a \rho V_a^2 / 2 \quad (9)$$

where f_a is the air friction coefficient, ρ is the air density and V_a is average air velocity over the wing. The velocity in the film at height z is

$$u = \tau z / \mu \quad (10)$$

where μ is the fluid viscosity.

The flow was calculated by use of the u momentum equation,

$$\frac{du}{dt} = \gamma \frac{\partial^2 u}{\partial z^2} \quad (11)$$

and the continuity equation,

$$\frac{\partial w}{\partial z} = \frac{\partial u}{\partial z} \quad (12)$$

ORIGINAL PAGE IS
OF POOR QUALITY

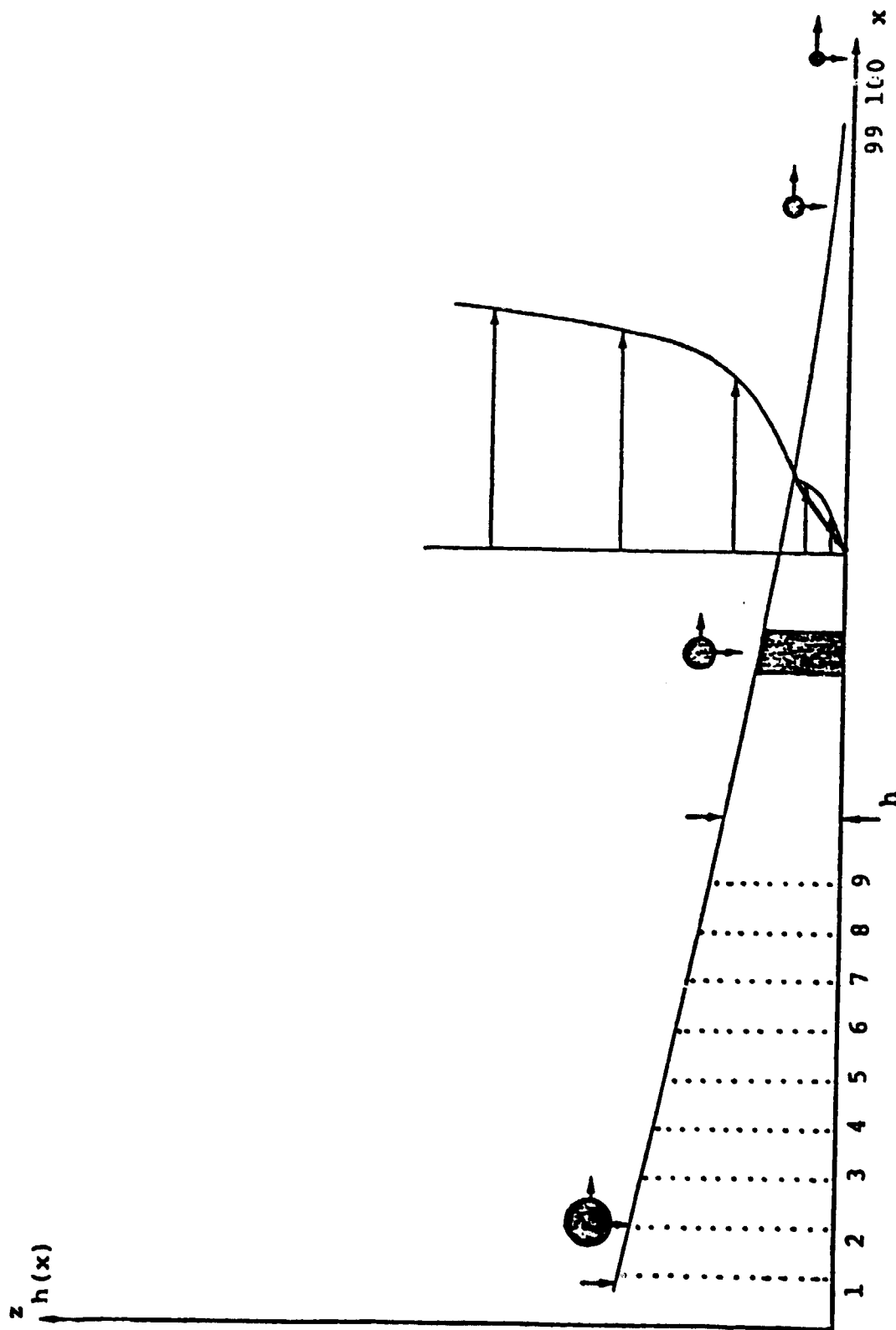


Figure 10. Water Film Thickness Model (2).

The calculation begins at the second station. Vertical velocities, w , are obtained from eq. (12) and u velocity tendencies from (11) beginning at one point below the film top and proceeding downward to one station above the bottom. This procedure is repeated sequentially through the 99th station and its completion constitutes one time step. Using a sufficiently small time step to ensure computational stability, the u velocity at time $t + \Delta t$ is calculated from

$$u(t+\Delta t) - u(t-\Delta t) = 2\Delta t \left[-u \frac{\partial u}{\partial x} - w \frac{\partial u}{\partial z} + \nu \frac{\partial^2 u}{\partial z^2} \right] \quad (13)$$

For the first time step a forward difference is used. Two neighboring stations make up a volume into which and out of which there is mass flux due to the arriving rain and film flow.

The mass balance at a station, i , may be expressed as

$$\frac{dm_i}{dt} = \frac{\rho_w}{A} \int_{z=0}^{z=h} u dz \Big|_{x=i\Delta x} - \frac{\rho_w}{A} \int_{z=0}^{z=h} u dz \Big|_{x=(i+1)\Delta x} + \frac{\partial m_i}{\partial t} \quad (14)$$

(1) (2) (3)

where terms 1 and 2 represent respectively mass flux into the i th station ($x=i\Delta x$) of Area A and out of the station ($x=(i+1)\Delta x$) due to film flow. Term 3 represents mass flux, into the i th station due to rain.

A change of mass is calculated from Eq. (14).

A new film thickness, h_i , results from

$$h_i = \frac{m_i + \frac{dm_i}{dt} \Delta t}{\rho_w A} \quad (15)$$

The procedure is repeated for each station from first to last. The calculations were performed from an initial time $t=0$ with an initial m_i corresponding to an initial thickness of 0.5 mm

until steady state was established. Other initial values of m_1 did not significantly change the steady state value.

The resulting average film thicknesses for the top of the airfoil derived by the model by rainfall rate are summarized in Table 3. The calculations were made for a symmetric airfoil of chord length 10 m at 0° angle of attack and 65 m/sec (126 knots) free stream airspeed. The value shown in Table 3 is an average representation of the film thickness throughout the airfoil segments.

The film thickness for the fuselage was estimated from calculations for an airfoil. Because of increased surface area of the fuselage in relation to its projected area, the droplet impact density on the fuselage is approximately 2/3 that on the airfoil. Thus, the mass impact rate per unit area on fuselage is only 2/3 that of the airfoil. The fuselage film thickness at a given rainfall rate is estimated as the airfoil film thickness that corresponds to 2/3 the given rainfall rate.

TABLE 3

AVERAGE FILM THICKNESS FOR A SYMMETRIC AIRFOIL AND FUSELAGE AT 0° ANGLE OF ATTACK, 10m CHORD

Rainfall Rate (mm/m)	Calculated Thickness Airfoil (mm)	Estimated Thickness Fuselage (mm)
100	≤ 0.2	≤ 0.2
200	≤ 0.5	≤ 0.2
500	0.8	0.6
1000	1.0	0.9
2000	1.3	1.1

SECTION 7
WEIGHT PENALTY

The weight penalty is due to a water film on the surface of the aircraft. Using a 747 as an example with the average film thicknesses calculated in Table 3, the weight penalties by rainfall rate are shown in Table 4. The values are for a film existing only on the top half of the wing and fuselage surfaces. Film thickness was not calculated for the lower surface, below the stagnation point. If a film exists there, it would be expected to be thinner because of a decreased water impact rate. Even assuming the film on the underside was equally thick it would only double the weight shown in Table 4. For a 747 aircraft whose landing weight is on the order of 180,000 kg, the maximum weight penalties cannot be much larger than 1% of landing weight. A 1% added weight has a negligible effect on aircraft landings.

TABLE 4
WATER MASS ON ALL AIRCRAFT SURFACES FOR VARIOUS RAINFALL RATES

Weight Penalties		
Aircraft = B747, Velocity = 126 kts, $\alpha = 0^\circ$		
Rainfall Rate (mm/hr)	Film Weight, top (kg)	Film Weight, top and bottom (kg)
100	---	---
200	7.33×10^2	1.47×10^3
500	1.17×10^3	2.34×10^3
1000	1.47×10^3	2.94×10^3
2000	1.94×10^3	3.88×10^3

SECTION 8

AIRFOIL ROUGHNESS

An airfoil or fuselage in heavy rain may be roughened in at least three ways: (a) waves develop in a water film clinging to the wings and fuselage, (b) in the absence of a liquid film, globules dot the wing surface and are blown back by wind stress, (c) drops impacting a water film disturb its surface.

This study has analyzed two of the roughness sources. They are the roughening of a water film on an airfoil's top surface due to drop impacts and the roughness due to waves in the water film. Future modeling can consider the possibility of blow back of liquid water globules.

8.1 ROUGHNESS DUE TO IMPACT

We have investigated the impact of a raindrop on a thin film in order to evaluate its contribution to roughening an airfoil. The assessment of raindrop splashes is based on the work of Machlin and Metaxas (1976) who investigated the craters formed when a water drop impacts a thin water film. Unfortunately their investigation was conducted at drop velocities slower than the impact velocity of raindrops on an aircraft wing. Thus extrapolation of their results to higher velocities was required.

The raindrop splash model assumes that a drop hitting a thin film forms a cylindrical crater. All the water originally residing within the crater is assumed to go into the crater crown. Virtually no wave swell results from the impact. An energy balance equation relating the non-dimensional crown height to crown radius in terms of the inertial, gravitational (Froude Number) and surface tension (Weber Number) is given by:

(Macklin and Metaxas, 1976)

$$(H^*)_{\text{theor}} = \frac{1 + 6(W_b)^{-1} + 2(F_N)^{-1} - 3(W_b)^{-1} D^* R_c^*}{6(W_b)^{-1} R_c^*} \quad (16)$$

where

$W_b = \rho_w R_d V_{\text{free}}^2 / \sigma$	Weber Number (ratio of inertial to surface tension force)
$F_N = V_{\text{free}}^2 / g R_d$	Froude Number (ratio of inertial to gravitational force)
$D^* = h / R_d$	Dimensionless depth of liquid film
$H^* = H / R_d$	Dimensionless crown height
$R_c^* = R_c / R_d$	Dimensionless crown radius
$t^* = V_{\text{free}} t / R_d$	Dimensionless time
$R_d = \text{drop radius}$	
$\sigma = \text{surface tension}$	

This equation does not take into account viscous forces (which contribute less than 7 percent) and other influences not accounted for in this idealized model. In comparing this model with experimental data Macklin and Metaxas found the model to account for 40 to 60 percent of the energy dissipation in shallow film impacts. The unaccounted energy is thought to predominately consist of surface energy. The solution of Eq. (16) requires the use of an empirical relationship between dimensionless crown heights, H^* , and crown radius, R_c^* . Figure 11 shows the ratio of H^*/R_c^* for different Weber numbers. It was necessary to extrapolate the curve from Figure 11 to much higher Weber numbers for application to drops impacting on an aircraft. An extrapolated ratio of 2.9 was used for a Weber Number of approximately 5×10^4 . Use of such a severely extrapolated value was undesirable but necessary. Some consolation can be gained by a sensitivity analysis using other ratios of H/R_c . Using ratios of

— Linear Regression Fit
••••• Macklin and Metaxas Data

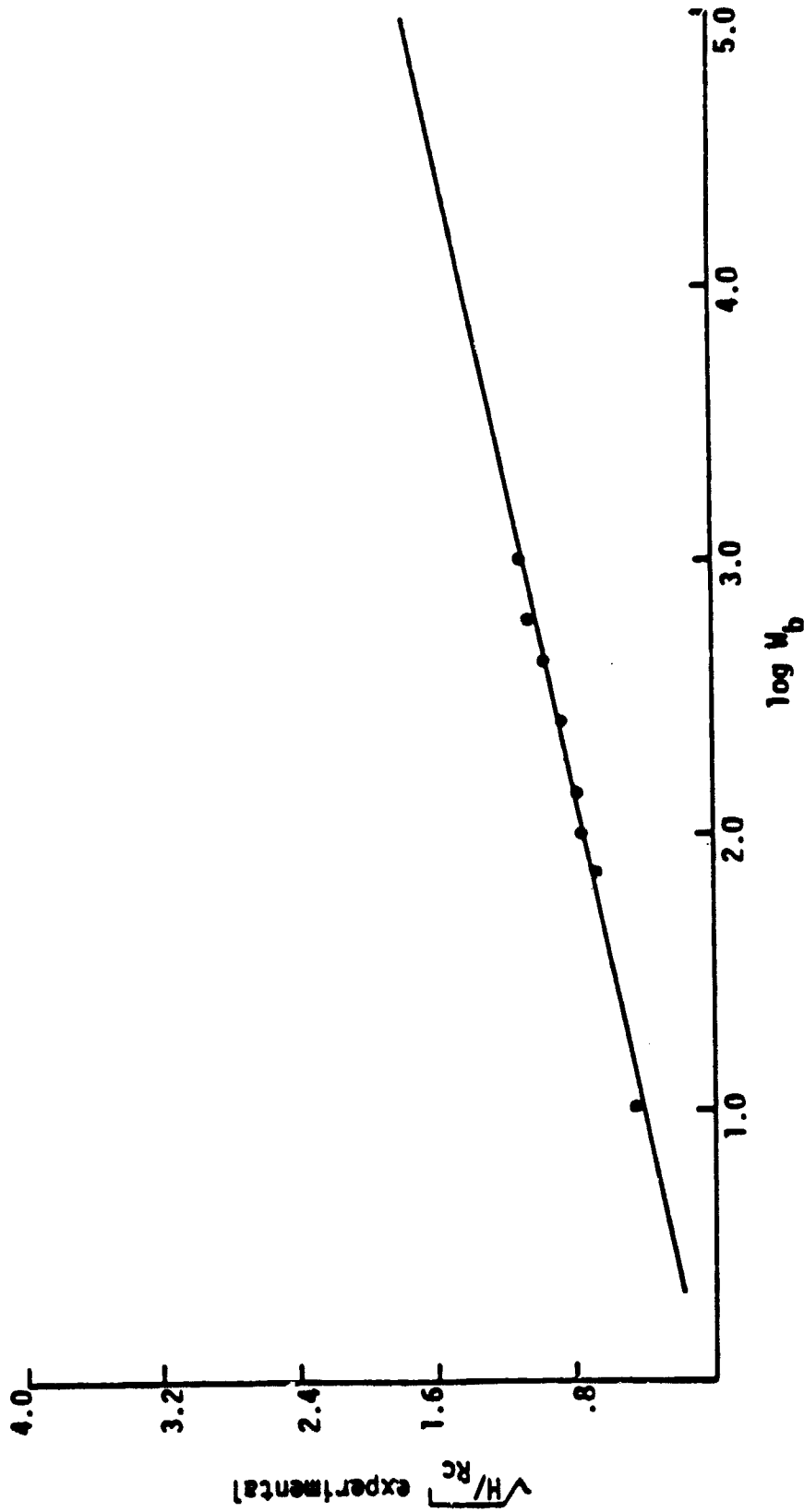


Figure 11. Ratio of Crown Height, H, to Cavity Radius at Maximum Crown Height as a Function of Weber Number using Macklin and Metaxas (1976) data.

$H/R_c = 1$ and $H/R_c = 5$ does not change the essential results of the analysis. Using the extrapolated ratio, H^* is theoretically obtained from the solution of Eq. (16). The theoretical crown height is then adjusted by Figure 12 to account for the energy dissipated that is unexplained by the model.

The dimensionless time to reach maximum crown height is obtained from Figure 13 as a function of experimental and theoretical values of H^* . Figures 11, 12, and 13 each required severe extrapolation of the experimental data for the situation of rain impacting on an airplane.

The values derived for maximum crown height, radius, and time to reach maximum height are the basic parameters for deriving the aerodynamic roughness height due to drop impacts on an airfoil. Table 5 shows these parameters for a drop impact velocity representative of a transport aircraft landing.

TABLE 5
DROP IMPACT PARAMETERS BY DROP SIZE
V=65M/sec

Drop Radius (mm)	W_b	F_N	H/R_c emp	H^* theor	H^* emp	t_c^*
0.5	2.98×10^4	8.61×10^5	2.79	113.94	13.2	41.5
1.0	5.79×10^4	4.31×10^5	2.98	169.48	14.6	43.4
2.0	1.16×10^5	2.15×10^5	3.25	250.35	15.8	45.0
4.0	2.31×10^5	1.08×10^5	3.53	368.71	16.8	46.0

Evaluating the roughness of a film due to drop impacts requires knowing two parameters. One parameter is the mean

ORIGINAL FILED IN
OF POOR QUALITY

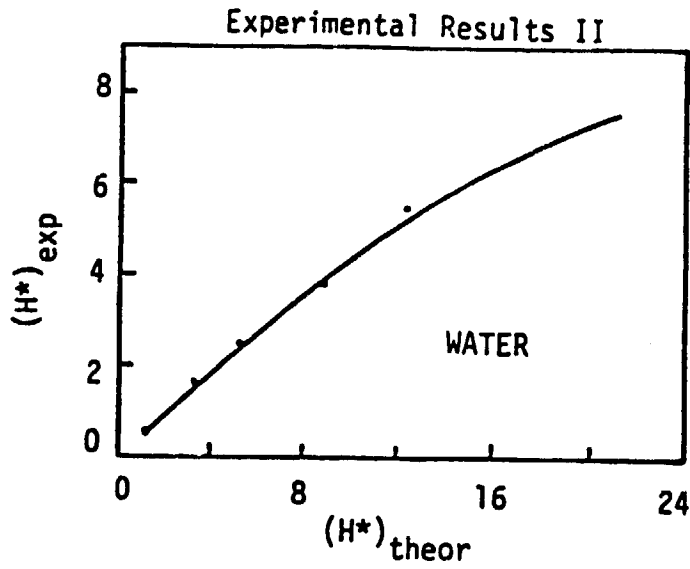


Figure 12. Dimensionless Crown Height as a Function of Theoretical Values from (16). (After Macklin and Metaxas, 1976).

ORIGINAL PAGE IS
OF POOR QUALITY

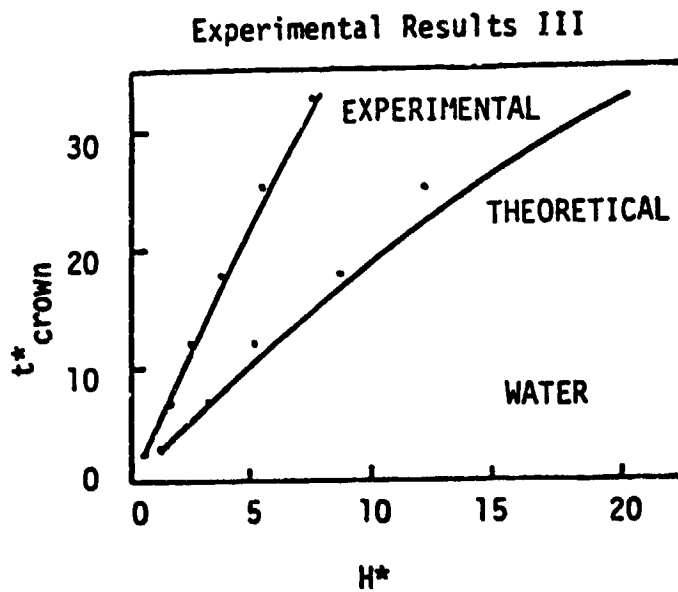


Figure 13. The Dimensionless Time to Reach Maximum Crown Height t^*_{crown} as a Function of the Theoretical and Experimental Values of H^* for Shallow Liquid Splashing. (After Macklin and Metaxas, 1976).

height of a drop impact crown throughout its life cycle from formation to dissipation. The other parameter is the mean separation distance between drop impacts. Both parameters can be calculated from the results in Table 5 and local collection efficiencies.

The mean separation distance is derived from the rate of drop impacts and the time over which a drop impact persists. The rate of drop impacts of diameter D at a given location on the airfoil is the product of drops per unit volume times the freestream air speed times the local collection efficiency. The time period, Δt , over which a drop impact crater exists is conservatively approximated as twice the time required for a crater to reach maximum crown height, that is:

$$\Delta t = t_c^* D / V_{\text{free}} \quad (17)$$

The number of drop impact crowns of diameter D occurring at any given time is

$$N(D) V_{\text{free}} \Delta t \beta = N(D) t_c^* \beta D \quad (18)$$

where $N(D)$ is number of drops of diameter D per unit volume in free air. Using the Marshall-Palmer distribution to represent $N(D)$ and integrating the above over all D gives the total number of drop impact craters at a given time,

$$N = \int_{D=0}^{D=\infty} N_0 e^{-\psi D} t_c^* \beta D dD = \frac{N_0 t_c^* \beta}{\psi^2} \quad (19)$$

In integrating eq. (19) both t_c^* and β are assumed constant as they are slowly varying functions of D .

The mean separation distance is given as the inverse square root of the number of drops involved in an impact at any instance of time per unit area. That is:

$$\bar{D} = \frac{1}{\sqrt{N}} \quad (20)$$

For a drop of diameter D , the average drop impact crown height over its lifetime is conservatively approximated as one half of its maximum crown height. That is:

$$k(D) = \frac{H_{\text{exp}}^* D}{4} \quad (21)$$

The average height, \bar{k} , for a population of drop impact craters of varying diameters is the population weighted mean

$$\bar{k} = \frac{\int_{D=0}^{D=\infty} k(D)N(D)dD}{\int_{D=0}^{D=\infty} N(D)dD} \quad (22)$$

The evaluation of eq. (22) again assumes t_c^* and β are constant and that $N(D)$ is represented by a Marshall-Palmer distribution. Thus,

$$\bar{k} = \frac{H_{\text{exp}}^* D}{2\psi} \quad (23)$$

where \bar{k} is considered to be the height of the roughening elements produced by drop impacts.

8.1.1 Sandgrain Roughness

The roughness height is estimated from Eqs. (20) and (23) by finding the equivalent sand grain roughness (Dirling, 1973). We first found the ratio A_p/A_s , where A_p is the projected area of drop crowns in the freestream velocity direction and A_s is the windward surface area of the element as seen by the flow. We estimate this ratio to be about 0.64 for cylindrical drop impact crowns. From Dirling, Λ is correlated in terms of the spacing parameter, \bar{D}/\bar{k} , as

$$\Lambda = (\bar{D}/\bar{k})(A_p/A_s)^{-4/3} \quad (24)$$

Considering, for simplicity, an average local collection efficiency of $\beta = .17$ for all rainfall rates, and using the value of t_c^* corresponding to the mean drop size for

a given rainfall rate, \bar{D} was calculated from (20) for a free stream velocity of 65m/sec and is given in Table 6.

TABLE 6
AVERAGE SPACING BETWEEN RAINDROPS BY RAINFALL RATE

Rainfall rate (mm/hr)	\bar{D} (cm)
100	20.16
200	17.43
500	14.38
1000	12.43
2000	10.74

Using the same assumption, the average geometric height of drop impacts was calculated for different rainfall rates using Eq. (23) as shown in Table 7.

TABLE 7
AVERAGE GEOMETRIC HEIGHT OF DROP IMPACTS BY RAINFALL RATE

Rainfall rate (mm/hr)	Height \bar{k} (mm)
100	4.8
200	5.6
500	6.7
1000	7.8
2000	9.0

From Dirling the correlation equations for sandgrain roughness developed from experimental data are:

$$\begin{aligned}
 k_s/\bar{k} &= 0.0164\Lambda^{3.7} & , \Lambda < 4.93 \\
 &= 139\Lambda^{-1.9} & , \Lambda > 4.93
 \end{aligned}
 \tag{25}$$

where k_s = equivalent sandgrain roughness.

The average sand grain roughnesses by rainfall rate derived by eqs. (24) and (25) are given in Table 8.

TABLE 8
SAND GRAIN ROUGHNESSES BY RAINFALL RATE

Rain rate (mm/hr)	k_s (mm)
100	0.18
200	0.37
500	0.89
1000	1.83
2000	3.65

8.1.2 Drag Increase Due to Impact Roughness

To make estimates of the drag increase due to these values of sandgrain roughness, results from Young (1965) for fixed roughness elements with turbulent flow over a flat plate were utilized. The mean friction coefficient, C_{FS} , for smooth wall flow is given by:

$$C_{FS} = 0.088/(\log Re - 1.5)^2 \tag{26}$$

In roughened flow the mean friction coefficient is:

$$C_{FR} = (1.89 + 1.62 \log L/k_s)^{-2.5} \tag{27}$$

where L is the mean aerodynamic chord or fuselage length. For a 747 wing, an appropriate Reynolds number in the landing configuration is $Re = 3.23 \times 10^7$ while for the fuselage it is 2.74×10^8 .

Using values of 8.3 meters for the Mean Aerodynamic Chord of a B747 and 70 meters as the fuselage length, the solution of Eqs. (26) and (27) are shown in Table 9.

TABLE 9
MEAN FRICTION COEFFICIENT FOR SMOOTH AND ROUGHENED AIRFOIL AND FUSELAGE

L = 8.3m Airfoil L = 70m Fuselage

Rain Rate mm/hr	C_{FS} Airfoil	C_{FR} Airfoil	C_{FS} Fuselage	C_{FR} Fuselage
100	.0024	.0036	.0018	.0025
200	.0024	.0042	.0018	.0028
500	.0024	.0051	.0018	.0033
1000	.0024	.0059	.0018	.0038
2000	.0024	.0069	.0018	.0043

An estimate of the influence of an increase in friction drag on total drag for the 747 aircraft in the landing configuration can be approximated as follows. For a 747 aircraft with 30 degrees flaps descending a glide slope at 2 degrees angle of attack, the basic drag coefficient including landing gear is approximately $C_{D_0} = .15$. The basic drag coefficient can be decomposed into contributions from airfoil and fuselage friction coefficients as:

$$C_{D_0} = 2C_{FS}^{air} + C_{FS}^{fus} A^{fus} / S + C_{D_0} \text{ etc} \quad (28)$$

where

A^{fus} = total surface area of the fuselage

S = wing area (upper surface)

$C_{D_0} \text{ etc}$ = all other factors that contribute to C_{D_0} .

The factor, 2, in the first term on the right hand side accounts for friction drag on both upper and lower wing surfaces. A representative value for the ratio of fuselage to upper wing surface area for a 747 aircraft is

$$\frac{A^{fus}}{S} = 3.4 .$$

For an aircraft whose upper surfaces are roughened by rain, the change in C_{D_0} due to increased friction drag is:

$$\Delta C_{D_0} = C_{FR}^{air} - C_{FS}^{air} + \frac{A^{fus}}{2S} C_{FR}^{fus} - C_{FS}^{fus} \quad (29)$$

Using the appropriate values from Table 9 in Eq. (26) the percent changes in C_{D_0} for a 747 aircraft in the landing configuration are shown in Table 10.

TABLE 10

INCREASE IN TOTAL DRAG DUE TO INCREASED WING AND FUSELAGE FRICTION DRAG. (747 AIRCRAFT LANDING CONFIGURATION)

Rainfall Rate (mm/hr)	$\Delta C_D / C_{D_0}$
100	1.6%
200	2.3%
500	3.5%
1000	4.6%
2000	5.9%

The increases in drag coefficient shown in Table 10 are small but significant. If both the upper and lower surfaces of fuselage and airfoil were roughened to the same extent, the values shown in Table 10 would increase by a factor of 2. Similarly, if the above analysis were performed on a smaller

aircraft, such as a 727 or DC9 a larger percentage increase in friction drag would be derived from eqs. (26) and (27).

To establish the validity of applying eq. (26) and (27), which refer to flat plate turbulent flow conditions to an airfoil with extended flaps, a comparison of theory to experimental wind tunnel measurements by Ljungstroem (1972) was made. Ljungstroem measured both lift and drag increments on a 2-dimensional wing section with and without high lift devices. The wing chord length was = 65 cm. Figure 14 shows C_D and C_L curves for a clean wing and a roughened wing (95% and 100% coverage) with various sand grain roughness elements. Using eqs. (26) and (27), the appropriate Reynolds number, $L = 65\text{cm}$ and $k_s = 0.1\text{mm}$, $k_s = 0.5\text{mm}$, the smooth and roughened friction coefficients were calculated as $C_{F_S} = .0036$, $C_{F_R} = .0052$ ($k_s = .1\text{mm}$) and $C_{F_R} = .0076$ ($k_s = .5\text{mm}$). The values are shown in Figure 14 after converting to drag coefficient. Note that Eq. (26) gives a good approximation to the smooth airfoil drag coefficient but Eq. (27) grossly underestimates the roughness penalty by a factor of 3 or more. Since the wind tunnel measurements include pressure drag as well as friction drag it is apparent that additional drag penalties result from roughness above those calculated by Eq. (27). Similar results were obtained from a comparison of Ljungstroem measurements on a high lift airfoil with 25-degree slats and 20 degrees flap. Figure 15 shows the measured C_D vs C_L at low angles of attack as well as the friction drag calculations using Eqs. (26) and (27). The experimentally derived increase in C_D between the clean and fully roughened airfoil is approximately $\Delta C_D = 0.025$ for $k_s = 0.5\text{mm}$ and $\Delta C_D = 0.009$ for 0.1mm roughness. Calculated differences in skin friction coefficient are $\Delta C_F = .0040$ for $k_s = 0.5\text{mm}$ and $\Delta C_F = .0017$ for $k_s = 0.1\text{mm}$. For this wing configuration the skin friction calculation underestimates the roughness induced drag increase by a factor of 5 to 6. Thus in applying the increase in

ORIGINAL CASE IS
OF POOR QUALITY

$Re = 2.6 \cdot 10^6$ CONFIG W

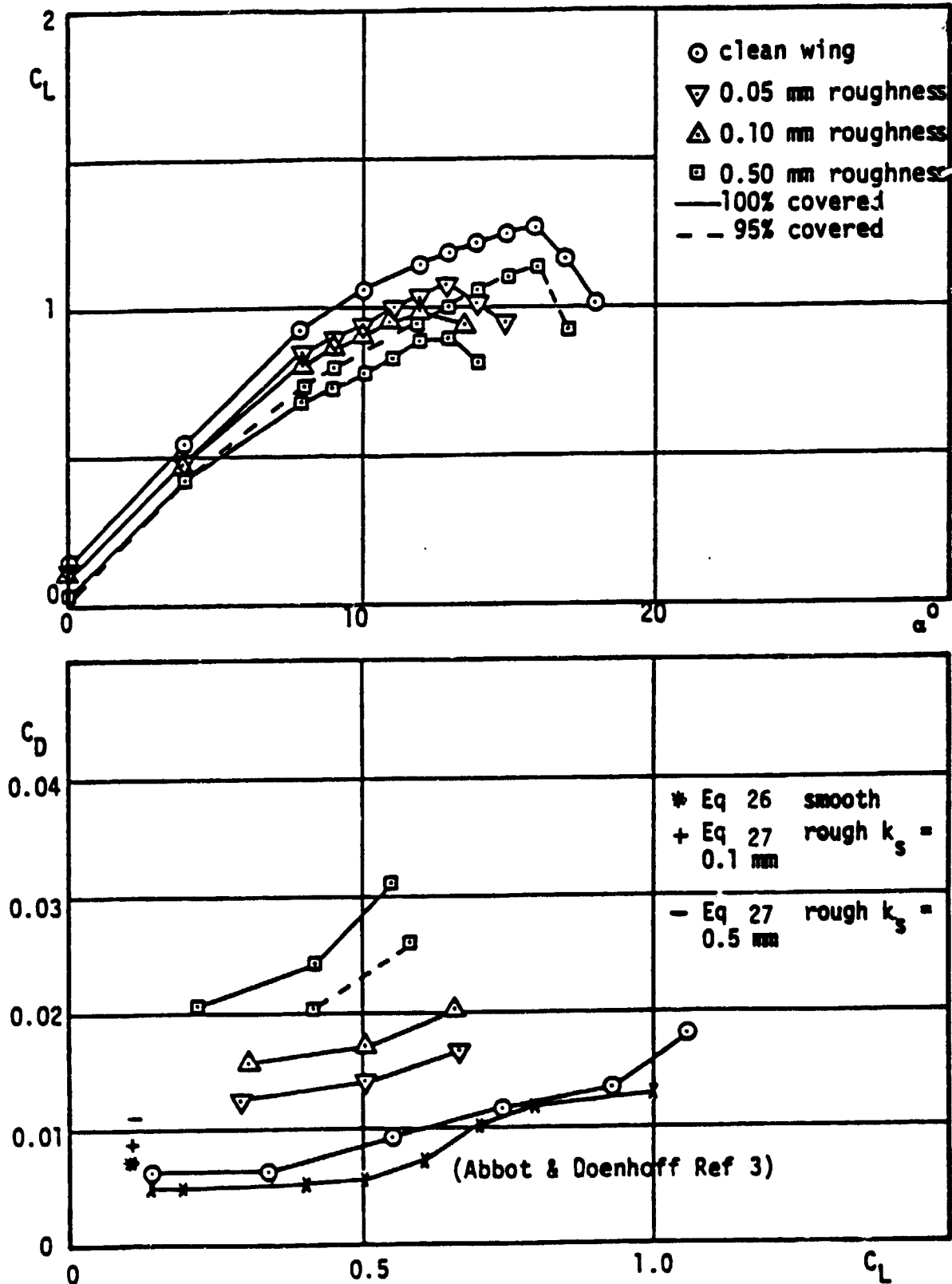


Figure 14. C_L and C_D for Configuration W.
Wing Section NACA 65 A-215. (After Ljungstroem;
1972).

ORIGINAL PAGE IS
OF POOR QUALITY

CONFIG WFS

Re = $2.6 \cdot 10^6$

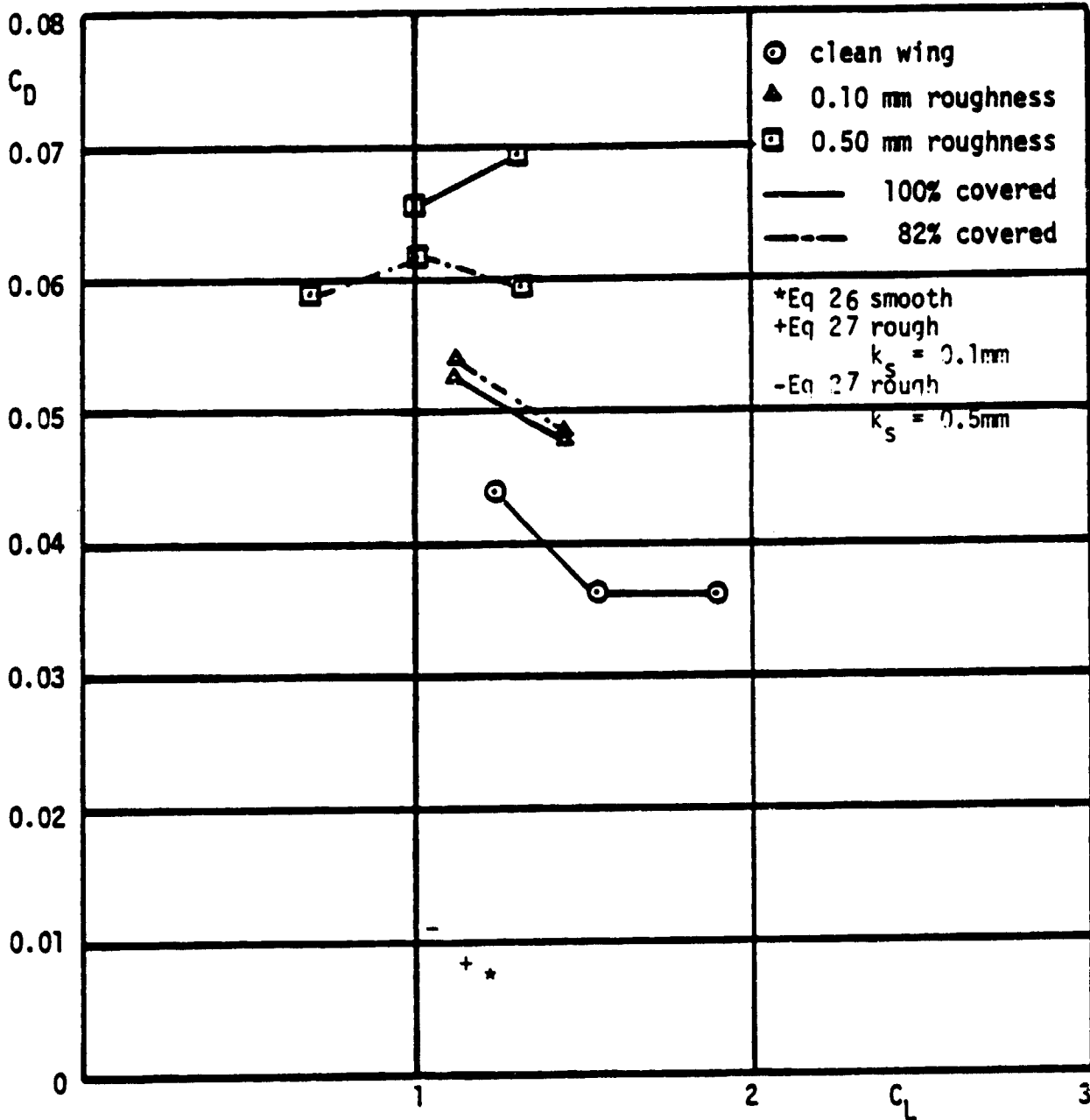


Figure 15. C_D vs C_L for Configuration WFS
Wing Section with Slat and Training Edge
Flap. (After Ljungstroem; 1972).

friction drag calculated by Eqs. (26) and (27) as the sole contributor to increased drag coefficient and underestimation by a factor of 3 to 6 appears likely. Consequently the percentage drag penalties due to roughness shown in Table 10 should be increased by a compensating factor - perhaps on the order of 3.

8.1.3 Summary of Impact Drag Penalties

The above results on drag penalties that arise from the roughness of an airfoil and fuselage due to rain drop impacts indicates aerodynamic penalties may exist. Numerous assumptions and experimental data extrapolation however were required to derive the overall drag penalty for a 747 aircraft. Most critical of these assumptions relate to the extrapolation of droplet crown height and the time to reach maximum crown height for Weber numbers far beyond the range of experimental measurements. Also the assumption of fixed roughness elements, no interaction of the airflow with the crown formation, and no shattering of the water drops prior to impact, may be important. Nonetheless the derived roughness heights when evaluated in comparison with experimentally derived drag penalties appear especially significant. Furthermore since the roughness due to the waviness of the water film has not yet been taken into account, a further contribution to the drag penalty may result. Finally, if the same analysis were performed on a smaller size transport aircraft there is reason to believe the drag penalty may increase.

8.2 ROUGHNESS DUE TO FILM WAVINESS

Surface waves are observed on water film surfaces under wind stress (Kapitza, 1964). They have been shown to have a comparable effect on airflow as sand roughened walls. Wurz (1978) conducted an experimental program to study the interference of a wavy liquid film with a turbulent gas boundary layer. Using a two-phased wind tunnel of .72 meters in length, and appropriate instrumentation, Wurz measured various properties of the water

film and its interface with the air boundary layer for a range of Mach numbers from subsonic to supersonic. Of interest to our application for rain roughness on an airfoil are the results at low subsonic Mach numbers. Tests conducted in the Mach number range of Mach = .18 to Mach = .6 produced film thickness in the range of .014 mm to .2 mm. The water flow rates associated with these film thicknesses are an order of magnitude less than that produced by an aircraft penetrating even a 300 mm/hr rainfall rate at landing speed. Thus, the results of the Wurz experimental work, even though it covers sufficiently low Mach numbers, must be extrapolated to thicker films than occurred in the experimental tests. Wurz's results however, indicate an increase in friction coefficient as the film thickness increases. A relationship was also established between the mean film thickness and equivalent sand grain roughness as derived from the roughness Reynolds number; this ratio varies from between 1.25 and 2.0 in the subsonic test range. Using a ratio of 1.5, an equivalent sand grain roughness was derived for the airfoil and fuselage film thicknesses associated with 100 mm to 2000 mm rainfall rates. Table 11 shows these results.

TABLE 11
EQUIVALENT SAND GRAIN ROUGHNESS OF WAVY WATER FILM

Rain Rate (mm/hr)	Equivalent Sand Grain Roughness k_g	
	Airfoil (mm)	Fuselage (mm)
100	<0.3	<0.3
200	0.7	0.3
500	1.2	0.9
1000	1.5	1.4
2000	2.0	1.7

Again using eq. (27), we estimated the increased skin friction coefficient. Table 12 shows these values for the airfoil and fuselage versus rainfall rate.

TABLE 12
INCREASE IN SKIN FRICTION DUE TO FILM WAVINESS

Rain Rate (mm/hr)	\bar{C}_{FR} Airfoil	\bar{C}_{FR} Fuselage
100	.0040	.0027
200	.0048	.0032
500	.0053	.0032
1000	.0055	.0036
2000	.0059	.0038

Using eq. (29) these increases in friction drag from Table 12 were converted to percent increase on drag coefficient for waves on the upper surface of the wing and fuselage. Table 13 shows these results.

TABLE 13
INCREASE IN DRAG COEFFICIENT DUE TO FILM WAVINESS

Rainfall Rate (mm/hr)	$\Delta C_D / C_{D_0}$ (%)
100	2.1
200	3.2
500	3.8
1000	4.2
2000	4.6

Drag increases in the range of two to five percent are derived for the various rainfall rates. This drag increase is based solely upon an increased friction coefficient derived from Eqs. (26), (27), and (29). If, however, the drag coefficient penalty was derived using the sand grain roughness calculation of Table 11, and the experimental measurements of Ljungstroem, then the drag penalties would increase by a factor of from two to six over those of Table 13. Thus there is reason to suspect that Table 13 may seriously underestimate the actual drag penalties associated with the waviness of the water film.

In comparing the derived drag penalty due to film waviness (Table 13) with that derived for drop impact cratering, (Table 10) it is seen that the impact cratering penalty is approximately the same as that associated with film waviness. However, the experimental data upon which the waviness calculations were based require less severe data extrapolation and thereby more confidence is placed in these values. In combining the drag estimates due to waviness with those due to drop impact cratering and taking into account the possible underestimating of these penalties when compared to experimental measurements, a best

overall estimate of total drag penalty for a transport aircraft in the landing configuration was made. We estimate this penalty for 100 to 2000 mm/hr rainfall rates to be in the range of ten percent at the lower rainfall rates up to 20 percent or more for the incredible rates.

8.3 REDUCTION OF LIFT DUE TO ROUGHNESS

Distributed roughness on the upper surface of an airfoil also affects lift. Brumby (1979) summarized the results of 23 experimental investigations concerning the effect of roughness on lift coefficient and stall angle. Included in Brumby's analysis was the data of Ljungstroem for airfoils with and without high lift devices (see Figure 4). For a fully rough airfoil with "large" roughness elements, the lift coefficient was found to decrease at all angles of attack. For "medium" roughness a decrease in the lift coefficient primarily occurs at high angles of attack. The decrease in maximum lift coefficient (CL_{max}) is related to the ratio of roughness element height to wing chord. Decreases in CL_{max} as high as 30-40 percent occur for "large" roughness elements. A decrease in stall angle also accompanies a decrease in CL_{max} . A stall angle decrease of 4 to 5 degrees is appropriate to a decrease in CL_{max} of 30 to 40% while one to three-degree decreases in stall angle is appropriate for lift losses of 5 to 15%. An increase in stall speed also occurs. Stall speed increases of 10 to 20 knots accompany a loss in maximum lift of 10 to 30%. For a roughened airfoil, the drag coefficient increases dramatically at high angles of attack because of the premature onset of stall.

Using the results of Brumby, estimates were made of the reduction in maximum lift and increase in stall angle for a rain roughened airfoil in a landing configuration.

Using the sand grain roughnesses associated with drop impact from Table 8 and those associated with film waviness from

Table 11, the reduction in maximum lift coefficient and in angle of attack at stall were calculated. These calculations were derived from Brumby's curve for an airfoil with high lift devices retracted whose entire upper surface is roughened.

TABLE 14
REDUCTION IN MAXIMUM LIFT COEFFICIENT AND
ANGLE OF ATTACK AT STALL DUE TO ROUGHNESS

Rain Rate (mm/hr)	Drop Impact Cratering $\Delta\alpha_{CL_{max}}$	Film Waviness (%)	Drop Impact Cratering $\Delta\alpha_{CL_{max}}$	Film Waviness
100	7%	11	1-2°	1-3°
200	13%	20	1-3°	2-4°
500	25%	25	2-5°	2-5°
1000	29%	28	3-5°	3-5°
2000	34%	30	3-6°	3-5°

Brumby states however, that leading edge high lift devices even in the extended position do not recover degraded lift due to large amounts of roughness.

Table 14 shows a significant reduction of maximum lift and stall angle for roughness associated with both drop impact cratering and film waviness. Though unvalidated assumptions were necessary in deriving these results, we believe they are sufficiently realistic to warrant a most serious consideration of the influence of heavy rain on aircraft aerodynamics. Even the magnitude of lift penalties and stall angle decreases due to film waviness alone--for which our assumptions are best justified--could provide serious aerodynamic problems for an aircraft executing a go-around in a heavy rain environment. It is also likely that because of the decrease in stall angle, an aircraft may actually stall before activation of a stall warning device that is based upon clean airfoil aerodynamics.

SECTION 9
AIRCRAFT LANDINGS IN HEAVY RAIN

We modified an existing digital aircraft landing model (Luers and Reeves, 1973) to evaluate the effect of heavy rain upon aircraft landings. Each landing begins at 500 feet altitude where the aircraft is trimmed by determining the values of angle of attack, throttle setting, and elevator deflection, so as to result in unaccelerated flight down a 2.7° glide slope. The equations of motion were then integrated by a fourth order Runge-Kutta scheme. For no rain, the aircraft flies down the glide slope at a constant velocity until it reaches the ground. An aircraft encountering heavy rain no longer adheres to the glide slope because of momentum and drag penalties due to the heavy rain. The impact of heavy rain imparts a reverse thrust to an aircraft which decreases its airspeed. The rain roughness produces a change in the aircraft drag coefficient. The resulting deviation in touchdown point represents the severity of heavy rain to landing aircraft.

Two of the equations of motion are derived by summing the forces parallel and perpendicular to V (velocity vector relative to the earth) and applying Newton's Laws of Motion (Luers and Reeves, 1973). An additional term in the equation is necessary to represent momentum loss due to the heavy rain impact. In the parallel direction the term:

$$F_x \text{RAIN} = \cos\gamma F_x + \sin\gamma F_z \quad (30)$$

and in the perpendicular direction, the term

$$F_z \text{Rain} = -\cos\gamma F_z - \sin\gamma F_x \quad (31)$$

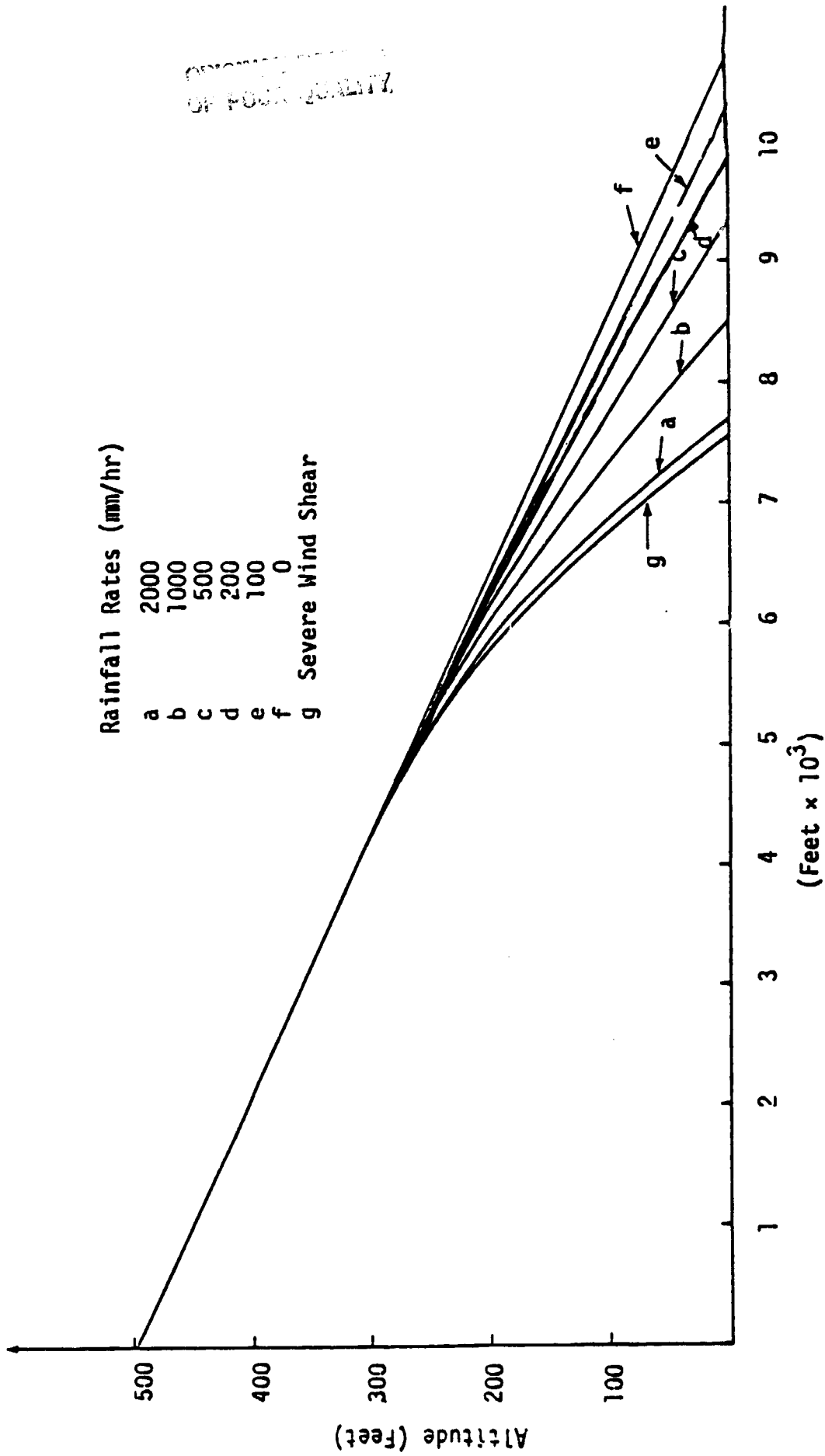
is added to the equation of motion where where γ is the flight path angle and F_x and F_z are the horizontal and vertical components of the rain momentum. The rain induced drag penalties

were introduced into the landing simulation by increasing the drag coefficient of the aircraft.

Fixed stick landing simulations were conducted using the aerodynamic data for a 747 aircraft and the influence of the rain momentum and roughness drag effects were evaluated. No lift penalties were introduced.

Figure 16 shows the trajectories of Boeing 747 landings with only momentum effects (Table 2) for five rainfall rates (2000mm/hr, 1000mm/hr, 500mm/hr, 200mm/hr, 100mm/hr). No drag penalty is included in these simulations. Also shown is a fixed stick trajectory for a landing in severe wind shear. Without rain or wind, the aircraft touches the ground in 10,593 feet. With a rain of 2000mm/hr, the shortfall is 2963 feet; for a 1000mm/hr rain, the shortfall is 2051 feet; for a 500mm/hr rain, the shortfall is 1211 feet; for a 200mm/hr rain, the shortfall is 525 feet; and for a 100mm/hr rain, the shortfall is 255 feet. The severe wind shear trajectory resulted from the wind profile shown in Figure 17; a strong vertical wind shear of at least 9 knots/100 feet. The momentum penalty under an incredible rainfall rate does not equal the severe wind shear penalty, nevertheless, the momentum penalty is significant for rainfall rates approaching 500mm/hr and above.

Figure 18 compares the trajectories of Boeing 747 landings incorporating only the drag penalties due to heavy rain for five rainfall rates with the severe wind shear landing and with a landing without rain and wind. The total drag penalties were arbitrarily estimated by multiplying the sum of the friction drag penalties due to drop impact and waviness by a factor of 3 to account for other sources of drag increase as well as for partial roughening on the lower airfoil and fuselage surfaces. Without rain or wind, the aircraft reaches the ground in 10,593 feet. With a rain of 2000mm/hr, the shortfall is 3440 feet, for a 1000mm/hr rain the shortfall is 3226 feet, for a 500mm/hr rain



ORIGINAL RESEARCH
OF FOUR QUALITY

Figure 16. 747 Landings with Momentum Penalty Only. Rain Encountered at 300 Feet.

ORIGINAL PAGE IS
OF POOR QUALITY

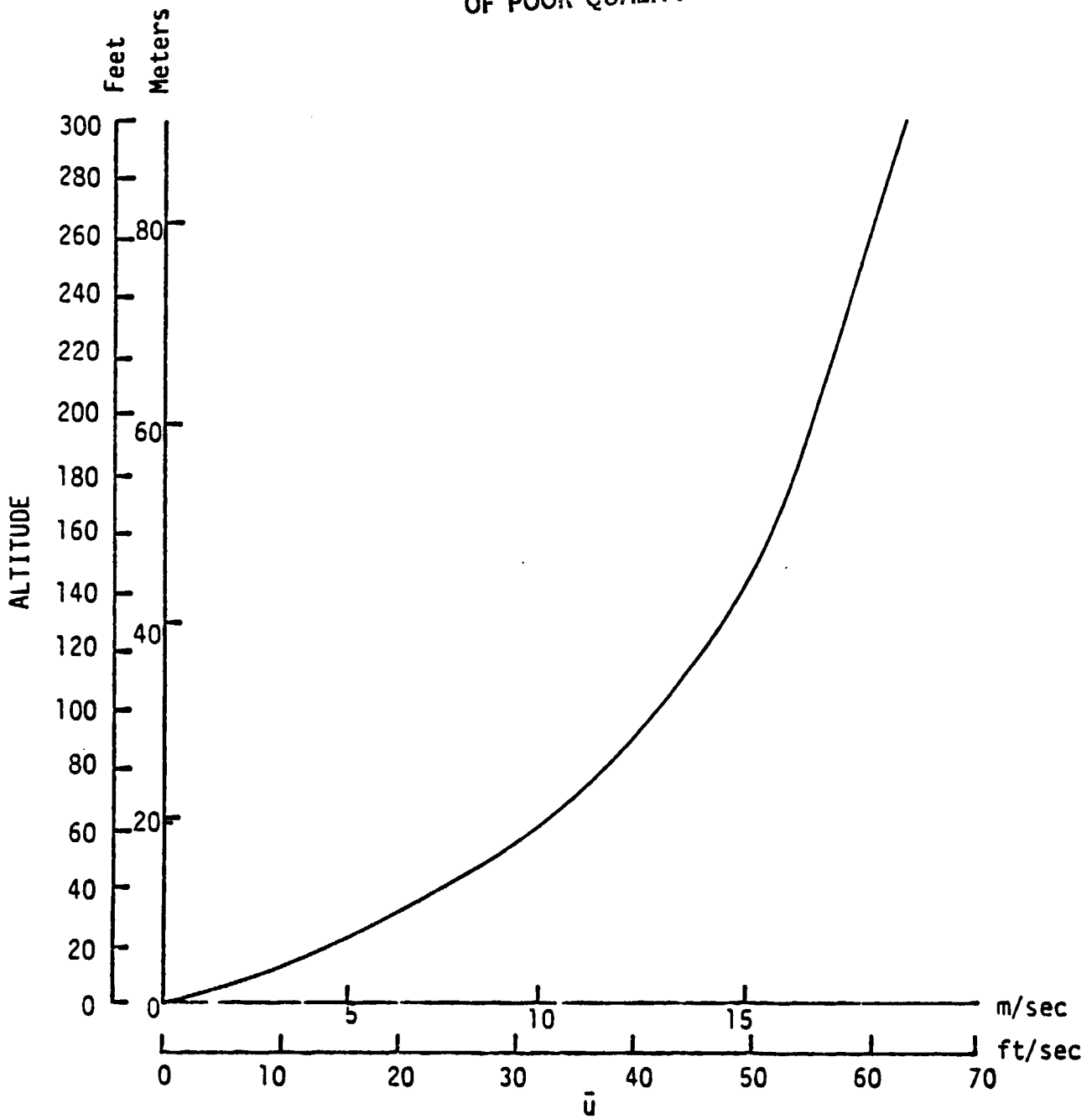


Figure 17. Wind Profile with Large Wind Shear.

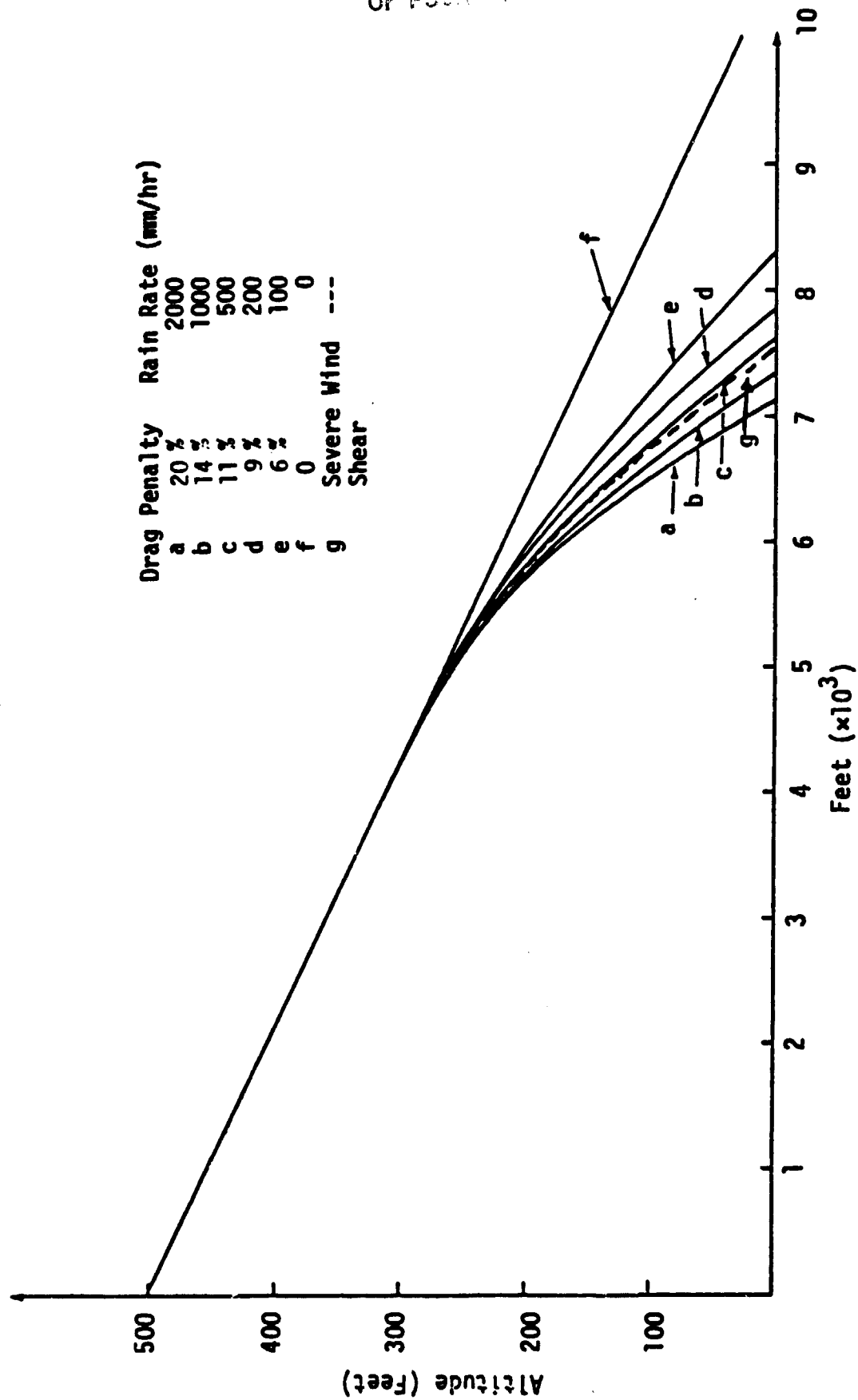


Figure 18. 747 Landings with Drag Penalty Only. Rain Encountered at 300 Feet.

the shortfall is 3000 feet, for a 200mm/hr rain the shortfall is 2704 feet, and for 100mm/hr the shortfall is 2245 feet.

For final comparison, both drag and momentum penalties from heavy rain are combined as shown in Figure 19. For a 2000mm/hr rain the shortfall is 3908 feet, for a 1000mm/hr rain it is 3562 feet, for a 500mm/hr rain it is 3219 feet, for a 200mm/hr rain it is 2832 feet, and for a 100 mm/hr it is 2343 feet. Under the assumed conditions a rainfall rate of approximately 400mm/hr would produce the same magnitude penalties of the severe wind shear shown in Figure 17. Table 15 summarizes these results.

In most cases, both heavy rain and severe wind shear will accompany each other. With both present, the shortfall is greater than with either absent. The increased shortfall is, however, not the simple addition of separate shortfalls arising from wind shear and from heavy rain.

LANDINGS WITH GENERAL AVIATION AIRCRAFT

To our knowledge, no general aviation (GA) aircraft crashes have been attributed to heavy rain. Heavy rain is not precluded, however, since it has not been possible to adequately identify and analyze crashes in which heavy rain was present. In addition, GA aircraft have been less likely to fly in severely degraded weather conditions due to pilot and instrument limitations. As more and more small aircraft become capable of instrument flying in poor weather, however, the likelihood for GA aircraft encounters with heavy rain will increase dramatically. Thus, an evaluation of the effect of heavy rain on GA landings is advisable.

The aerodynamic characteristics of a light single engine high-wing airplane (Greer, et al, 1973) were used in simulating the trajectory of a GA plane in heavy rain. The simulation was similar to that for a transport aircraft, as weight, momentum,

ORIGINAL QUALITY
OF POOR QUALITY

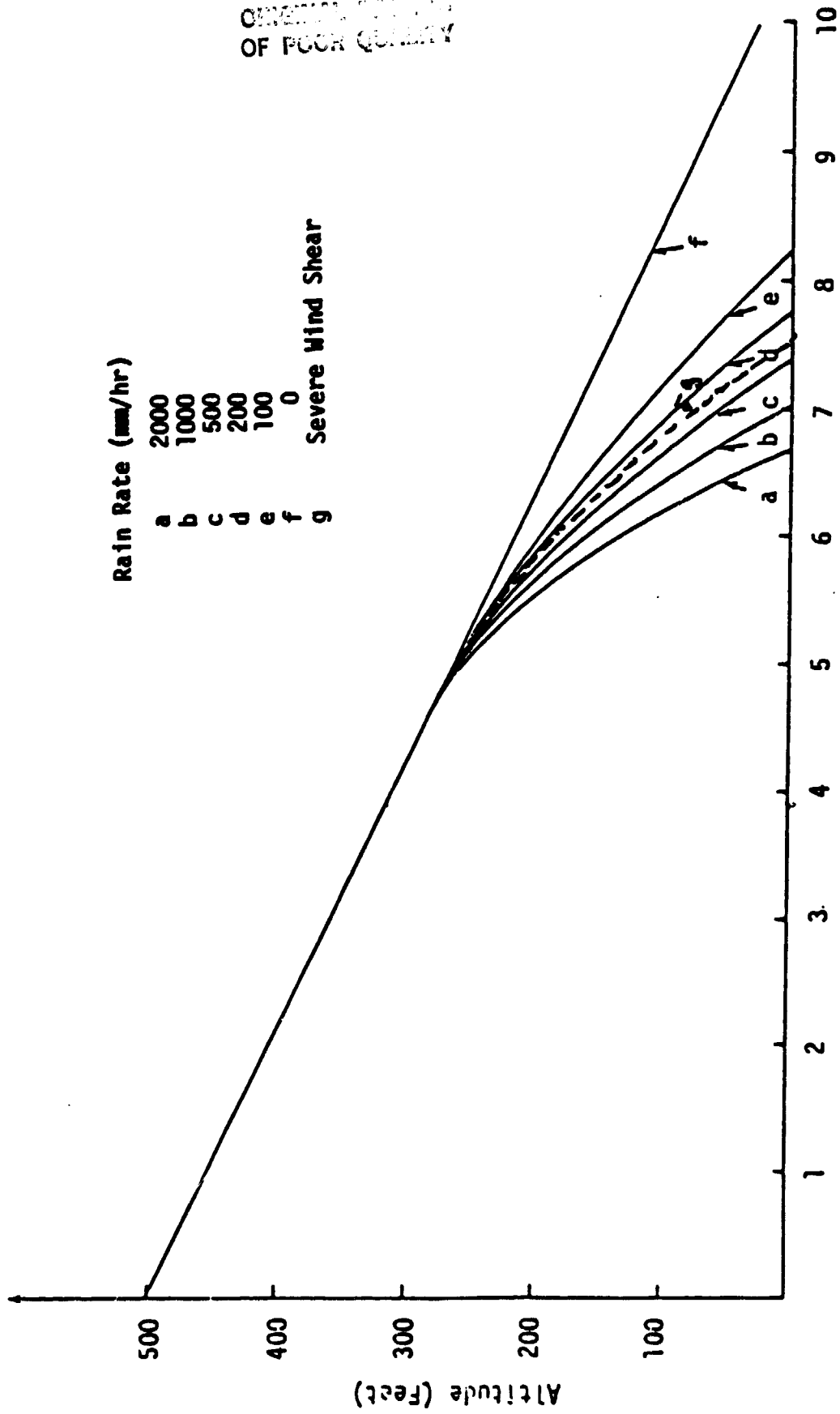


Figure 19. 747 Landings with Drag and Momentum Penalty. Rain Encountered at 300 Feet.

TABLE 15

SUMMARY OF LANDING SHORTFALLS (FEET) FOR A-747

Initial Height = 500 feet
 Glideslope = 10,593 feet
 Landing Weight = 400,000 lbs.
 Rain encountered at 300 feet.

Momentum Penalty Only

Rain Rate (mm/hr)	Shortfall
100	255
200	525
500	1211
1000	2051
2000	2963

Drag Penalty Only

Rain Rate (mm/hr)	Shortfall
100	2245
200	2704
500	3000
1000	3226
2000	3440

Weight Alone	Shortfall
1% Increase	72

Drag and Momentum Penalties Combined

Rain Rate (mm/hr)	Shortfall
100	2343
200	2832
500	3219
1000	3562
2000	3908

and drag penalties were separately evaluated under a fixed stick assumption.

The simulation results are similar to those for transport aircraft. The weight penalty is estimated to be less than 3% for a small plane; this causes a landing shortfall of less than 200 feet in a GA landing. The greater maneuverability of small aircraft makes such a shortfall negligible. Momentum and drag penalties are more severe for GA aircraft than for transport aircraft. In all cases, the smaller aircraft experiences somewhat greater landing shortfalls than transports.

The fixed stick assumption is not very realistic for a GA aircraft since their slower speeds and quicker responses provide greater maneuverability. Much greater latitude is available to the GA pilot for remedying penalties imposed by heavy rain than to the transport pilot. Nonetheless, the penalties imposed by heavy rain may create irrecoverably inhospitable flying conditions. More attention to realistic scenarios of GA aircraft in heavy rain is warranted.

SECTION 10 CONCLUSIONS

We have investigated some of the aerodynamic effects of rain on an aircraft. The weight penalty, loss of momentum due to rain impacts, and the increased drag and decreased lift due to droplet impact and waterfilm waviness have been considered. The weight penalty was found to be insignificant under normal landing conditions. The momentum penalty becomes significant for rainfall rates approaching 500mm/hr. Drag and lift penalties could be very significant for rainfall rates exceeding 100mm/hr. Landing simulations indicate that the drag and momentum penalties alone, associated with a 400 mm/hr rainfall rate, may be equivalent to that caused by a severe windshear of 9 knots/100 ft. In addition, lift penalties which were not included in the landing simulation, would cause even more performance deterioration.

It was necessary to make a number of approximations during the investigation. A conservative or realistic approach was used in contrast to a worst case analysis. For example, in estimating the momentum penalty of rain, both the deployment of flaps and the vertical velocity between plane and air were ignored. Both should increase aerodynamic penalties. We believe the estimates of aerodynamic penalties due to heavy rain, although crude, are sufficiently realistic to warrant concerned attention.

The significance of rain induced momentum loss is consistent with an antecedent investigation. Evidence for further aerodynamic degradation as a result of a rain roughened airfoil has been presented here. The combination of the two penalties have been shown comparable to strong windshear in degrading an aircraft landing trajectory. Normally, heavy rain will be accompanied by adverse winds. Separately neither may induce overly serious degradation while together both may be lethal.

A rain-roughened airfoil may cause a reduction of the maximum lift coefficient in addition to premature stall. With large

amounts of distributed roughness, such as may be caused by heavy rain, the deployment of leading edge high lift devices cannot reduce this effect. Finally, premature stall may occur insidiously before stall warning devices activate.

It appears likely that very heavy rain may have been a contributing factor in several aircraft accidents. Some of the loss in indicated air speed (IAS) appears to have been caused by rain. Thus, the derived windshears of accident reconstructions may be too large because rain was ignored. Future research will concentrate on refining the effect of rain on drag and assessing its effect on lift. In addition, the role of rain in several aircraft accidents will be addressed.

BIBLIOGRAPHY

- Ackley, S. F. and M. K. Templeton, Computer Modeling of Atmospheric Ice Accretion, CRREL Report 79-4, (1979), 36 pp.
- Bergrun, N. R., An Empirically Derived Basis for Calculating the Area, Rate, and Distribution of Water-Drop Impingement on Airfoils, NACA RN 1107, (1951), 1079-1099.
- Berry, E. X. and M. R. Pranger, "Equations for Calculating the Terminal Velocity of Water Drops," J. Appl. Meteor., 13, (1974), 108-113.
- Brumby, R. E., Wing Surface Roughness Cause and Effect, DC Flight Approach, McDonnell Douglas Corp., 32, (1979), 2-7.
- Dirling, R. B., Jr., A Method for Computing Roughwall Heat Transfer Rates on Re-entry Nosetips, AIAA paper 73-763, presented at the AIAA 8th Thermophysics Conference, Palm Springs, California, July 16-18, 1973.
- Greer, H. D., J. P. Shivers, and M. P. Fink, Wind-Tunnel Investigations of Static Longitudinal and Lateral Characteristics of a Full-Scale Mockup of a Light Single-Engine High-Wing Airplane. NASA TN D-7149, Washington, D.C., (1973), 157 p.
- Hartley, D. F. and W. Murgatroyd, "Criteria for the Breakup of Thin Liquid Layers Flowing Isothermally over Solid Surface," Int. J. of Heat and Mass Transfer, 7 (9), (1964), 1002-1015.
- Hershfield, D. M., "Estimating the extreme-value 1 Minute Rainfall," J. Appl. Meteor., 11, (1972), 936-940.
- Hess, J. L., Calculation of Potential Flow About Arbitrary Three-Dimensional Lifting Bodies. McDonnell Douglas Corp., Rep. No. MDC J5679-01, Oct. 1972.
- Jones, D. M. A., and A. L. Sims, "Climatology of Instantaneous Rainfall Rates," J. Appl. Meteor., 17, (1978), 1135-1140.
- Kapitza, P. L., "Wave Flow of Thin Layers of a Viscous Fluid," Collected Papers of P. L. Kapitza, New York, (1964), 662-709.
- Ljungstroem, B. L. G., Wind Tunnel Investigation of Simulated Hoar Frost on a Two-Dimensional Wing Section With and Without High Lift Devices, FFA-AU-902, Rapport AU-902, Aeronautical Research Inst. of Sweden, (1972), 32p.
- Lucey, G. K., A Rain Impact Analysis for an Artillery PD System, Harry Diamond Laboratories, TM-72-15, May, 1972.
- Luers, J. K. and J. B. Reeves, Effect of Shear on Aircraft Landing, NASA CR-1187, July, 1973.
- Macklin, W. C. and G. J. Metaxas, "Splashing of Drops on Liquid Layers," J. Appl. Phys., 9, (1976), 3963-3970.
- Markowitz, A. M., "Raindrop Size Distribution Expressions," J. Appl. Meteor., 15, (1976), 1029-1031.

Marshall, J. S. and W. McK. Palmer, "The Distribution of Raindrops With Size," J. Meteor., 5, (1948), 165-166.

Merceret, F. J., "Relating Rainfall Rate to the Slope of Raindrop Size Spectra," J. Appl. Meteor., 14, (1975), 259-260.

National Transportation Safety Board, Aircraft Accident Report, NTBS-AAR-76-8, Washington, D.C., (1975), 47 pp.

Norment, H. G., Additional Studies of the Effects of Airplane Flowfields on Hydrometeor Concentration Measurements, Air Force Geophysics Laboratory, Hanscom AFB, MA, Rep. AFGL-TR-76-0187, 1-56, AD-A032 311, (1976).

Rhode, R. V., Some Effects of Rainfall on Flight of Airplanes and on Instrument Indications, NACA, Rep. No. 803, (1941).

Riordan, P., Weather Extremes Around the World, Earth Sciences Laboratory, TR 70-45-ES, January, 1970.

Walsh, M. J., "Comment on 'Drag Coefficient of Spheres in Continuum and Rarefied Flows'," AIAA Journal, 14, (1977), 892-894.

Wurz, D., Subsonic and Supersonic Gas-Liquid Film Flows, AIAA 11th Fluid and Plasma Dynamics Conference, Seattle, WA. (1978).

Young, F. L., Experimental Investigation of the Effects of Surface Roughness on Compressible Turbulent Boundary Layer Skin Friction and Heat Transfer, DRL-532, CR-21, May, 1965.